



Metabolic implications of organelle–mitochondria communication

Isabel Gordaliza-Alaguero^{1,2,3} , Carlos Cantó^{4,5} & Antonio Zorzano^{1,2,3,*} 

Abstract

Cellular organelles are not static but show dynamism—a property that is likely relevant for their function. In addition, they interact with other organelles in a highly dynamic manner. In this review, we analyze the proteins involved in the interaction between mitochondria and other cellular organelles, especially the endoplasmic reticulum, lipid droplets, and lysosomes. Recent results indicate that, on one hand, metabolic alterations perturb the interaction between mitochondria and other organelles, and, on the other hand, that deficiency in proteins involved in the tethering between mitochondria and the ER or in specific functions of the interaction leads to metabolic alterations in a variety of tissues. The interaction between organelles is an emerging field that will permit to identify key proteins, to delineate novel modulation pathways, and to elucidate their implications in human disease.

Keywords contact sites; diabetes; endoplasmic reticulum; insulin resistance; lipid droplets

DOI 10.15252/embr.201947928 | Received 15 February 2019 | Revised 10 May 2019 | Accepted 28 May 2019 | Published online 14 August 2019

EMBO Reports (2019) 20: e47928

See the Glossary for abbreviations used in this article.

Contacts between mitochondria and other organelles

Mitochondria are highly dynamic and social organelles. They undergo continuous morphological changes to maintain cellular homeostasis; i.e., they fuse in response to specific physiological conditions, they divide to facilitate their removal by autophagy, and they maintain dynamic contacts with other membranous compartments of the cell. Mitochondria communicate with the endoplasmic reticulum (ER), lipid droplets (LDs), Golgi apparatus, lysosomes, melanosomes, and peroxisomes by establishing physical contacts (Fig 1). Fluorescent labeling of all these organelles *in vivo* has recently revealed cellular regions where three or more of these organelles physically interact [1]. Mitochondria and ER actively communicate, and their contact sites are important hubs for lipid

trafficking, mitochondrial dynamics, Ca^{2+} signaling, ER stress, apoptosis, and macroautophagy. Mitochondria–ER contact sites are also referred to as MERCs or when studied at a biochemical level MAMs (mitochondria-associated membranes). The contacts between mitochondria and LD functionally support triacylglyceride synthesis [2], and they are sustained by the interaction between MFN2 and PLIN1 [3]. Apposition of the Golgi apparatus and mitochondria has been demonstrated by microscopy techniques; however, the molecular features of this interaction remain poorly understood [4,5]. Mitochondria incorporate Ca^{2+} excess from the Golgi apparatus and have been proposed as a source of ATP for this organelle [4]. The contacts between mitochondria and lysosomes have been described to regulate mitochondrial fission, as well as lysosomal dynamics, by RAB7 GTP hydrolysis [6]. Melanosomes, which are lysosome-related organelles that store pigments, also interact with mitochondria [7]. These sites are associated with the process of melanogenesis [7]. MFN2 has been found at these areas of juxtaposition, and its knockdown reduces these interorganelle connections [7]. Peroxisomes and mitochondria interact through TOM20 in the mitochondria and ECI2 in peroxisomes. This interaction has functional implications in steroid biosynthesis in mouse Leydig cells [8]. Of all the mitochondrial contacts, those with ER are the best characterized to date, and some metabolic implications of those contacts have been also documented. The contacts between mitochondria and LDs or lysosomes are currently gaining insight and relevance and their potential metabolic implications are in the spotlight. In this review, we focus mainly on the molecular biology of mitochondria–ER, mitochondria–LD, and mitochondria–lysosome contacts and their involvement in metabolism.

Architecture of mitochondria–ER tethers

The structural scaffold of ER-mitochondria contact sites consists of proteins inserted in the outer mitochondrial membrane (OMM) that interact with those in the ER membrane. Available data indicate that ER bridging to mitochondria is governed by the following protein complexes (Fig 2): VAPB in the ER and PTPIP51 in mitochondria [9]; inositol 1,4,5-triphosphate receptors (IP3R1/2/3) in the ER and GRP75, together with VDAC1 in mitochondria [10]; BAP31 in the ER

1 Institute for Research in Biomedicine (IRB Barcelona), Barcelona Institute of Science and Technology (BIST), Barcelona, Spain

2 CIBER de Diabetes y Enfermedades Metabólicas Asociadas, Barcelona, Spain

3 Departamento de Bioquímica i Biomedicina Molecular, Facultat de Biologia, Universitat de Barcelona, Barcelona, Spain

4 Nestle Institute of Health Sciences (NIHS), Lausanne, Switzerland

5 School of Life Sciences, Ecole Polytechnique Fédérale de Lausanne (EPFL), Lausanne, Switzerland

*Corresponding author. Tel: +34 93 40 37197; E-mail: antonio.zorzano@irbbarcelona.org

Glossary

ABHD5	1-acylglycerol-3-phosphate O-acyltransferase	MFN1	Mitofusin 1
ACSL1	Acyl-CoA synthase long chain family member 1	MFN2	Mitofusin 2
AgRP	Agouti-related protein	MiD49/51	Mitochondrial dynamics proteins 49 and 51
AKT	Protein kinase B	MOSPD2	Motile sperm domain containing 2
ATAD3A	ATPase family, AAA domain containing 3A	MPTP	Mitochondrial permeability transition pore
ATF4	Activating transcription factor 4	mRNA	Messenger ribonucleic acid
ATF6	Activating transcription factor 6	mtDNA	Mitochondrial deoxyribonucleic acid
ATG12	Autophagy related 12	mTORC1	Mammalian target of rapamycin complex 1
ATG14	Autophagy related 14	mTORC2	Mammalian target of rapamycin complex 2
ATG16L1	Autophagy related 16 like 1	mTOR	Mammalian target of rapamycin
ATG5	Autophagy related 5	OMM	Outer mitochondrial membrane
ATGL	Adipose triglyceride lipase	OPA1	Optic atrophy 1
BAK	Bcl-2 homologous antagonist/killer	ORP5	Oxysterol-binding protein-related protein 5
BAP31	B-cell receptor-associated protein 31	ORP8	Oxysterol-binding protein-related protein 8
BAT	Brown adipose tissue	OSBP	Oxysterol-binding protein
BAX	BCL2-associated X	OXPHOS	Oxidative phosphorylation
BCL2	Apoptosis regulator B-cell lymphoma 2	PACS2	Phosphofurin acidic cluster sorting protein 2
BECN1	Beclin 1	PC	Phosphatidylcholine
BioID	Proximity dependent biotin identification	PDK4	Pyruvate dehydrogenase kinase 4
BiP	Binding immunoglobulin protein	PDZD8	PDZ domain-containing protein 8
Ca²⁺	Calcium	PEMT	Phosphatidylethanolamine N-methyltransferase
Ccl2	C-C motif chemokine ligand 2	PE	Phosphatidylethanolamine
CDIP	Cell death-inducing p53-target protein 1	PERK	Protein kinase RNA-like endoplasmic reticulum kinase
CEBPA	CCAAT/enhancer-binding protein alpha	PI3K	Phosphatidylinositol-3-kinase
CHOP	CCAAT/enhancer-binding protein homologous protein	PI4P	Phosphatidylinositol 4-phosphate
CIDEA	Cell death-inducing DFFA-like effector a	PLSD	Phosphatidylserine decarboxylase proenzyme
CYP11A1	Cytochrome P450 family 11 subfamily A member 1	PLIN1	Perilipin 1
CypD	Cyclophilin D	PLIN5	Perilipin 5
DRP1	Dynamin-related protein 1	POMC	Pro-opiomelanocortin
ECI2	Enoyl-CoA delta isomerase 2	PPARγ	Peroxisome proliferator-activated receptor gamma
elF2α	Eukaryotic initiation factor 2 alpha	PS	Phosphatidylserine
ER	Endoplasmic reticulum	PSS1	Phosphatidylserine synthase-1
ERK	Extracellular signal-regulated kinase	PSS2	Phosphatidylserine synthase-2
ERLIN2	ER lipid raft associated 2	PTPIP51	Protein tyrosine phosphatase interacting protein 51
ERMES	ER-mitochondria encounter structure	RAB5	Ras-related protein Rab-5
FACL4	Fatty acid-CoA ligase 4	RAB7	Ras-related protein Rab-7
FDB	Flexor digitorum brevis	ROS	Reactive oxygen species
FGF21	Fibroblast growth factor 21	RYR1/2/3	Ryanodine receptors 1, 2, and 3
FIS1	Mitochondrial fission 1	SEC61	Protein transport protein Sec61
FUNDC1	FUN14 domain-containing protein 1	SERCA	Sarco/endoplasmic reticulum Ca ²⁺ -ATPase
GLUT4	Glucose transporter type 4	SLC	Solute carrier protein
GM1	Gangliosidosis-1	SMP	Synaptotagmin-like mitochondrial-lipid-binding domain
GRP75	Glucose-regulated protein 75	SNAP23	Synaptosomal-associated protein 23
GRP94	Glucose-regulated protein 94	SREBP1C	Sterol regulatory element-binding protein 1
GTPase	GTP hydrolase	STARD1/3/4	Steroidogenic acute regulatory lipid transfer domain proteins 1, 3, and 4
GTP	Guanosine 5'-triphosphate	StAR	Steroidogenic acute regulatory protein
H₂O₂	Hydrogen peroxide	START	StAR-related lipid transfer
HDL	High-density lipoprotein	STX17	Syntaxin 17
HFD	High-fat diet	TAG	Triacylglycerides
IL6	Interleukin 6	TBC1D15	TBC1 domain family member 15
IMM	Inner mitochondrial membrane	TCHP	Trichoplein
INF2	Inverted formin 2	TG2	Transglutaminase 2
IP3R1/2/3	Inositol 1,4,5-triphosphate receptors 1, 2 and 3	Tnfa	Tumor necrosis factor alpha
IRE1α	Inositol-requiring enzyme 1 alpha	TOM20	Translocase of outer mitochondrial membrane 20
JNK	c-Jun N-terminal kinase	TOM22	Translocase of outer mitochondrial membrane 22
LC3	Microtubule-associated protein 1A/1B-light chain 3	TOM40	Translocase of outer mitochondrial membrane 40
LD	Lipid droplet	TOM70	Translocase of outer mitochondrial membrane 70
M1	Classically activated macrophages	TSPO	Translocator protein
MAM	Mitochondria-associated membranes	UCP1	Uncoupling protein 1
MAPK	Mitogen-activated protein kinase	UPR	Unfolded protein response
MCU	Mitochondrial calcium uniporter	VAMP4	Vesicle-associated membrane protein 4
MDV	Mitochondria-derived vesicle	VAPB	VAMP-associated Protein B
MEF	Mouse embryonic fibroblasts	VDAC1	Voltage-dependent anion channel 1
MEK	Mitogen-activated protein kinase kinase	VDAC2	Voltage-dependent anion channel 2
MERC	Mitochondria-ER contact sites	VDAC	Voltage-dependent anion channels
MFF	Mitochondria fission factor		

Glossary (continued)

VPS13A	Vacuolar protein sorting-associated protein 13 A
VPS15	Vacuolar protein sorting-associated protein 15
VPS34	Vacuolar protein sorting-associated protein 34
Vps39	Vacuolar protein sorting-associated protein 39

WASF3	Wiskott–Aldrich syndrome protein family member 3
WAT	White adipose tissue
XBP1	X-box binding protein 1
Ypt7	GTP-binding protein YPT7

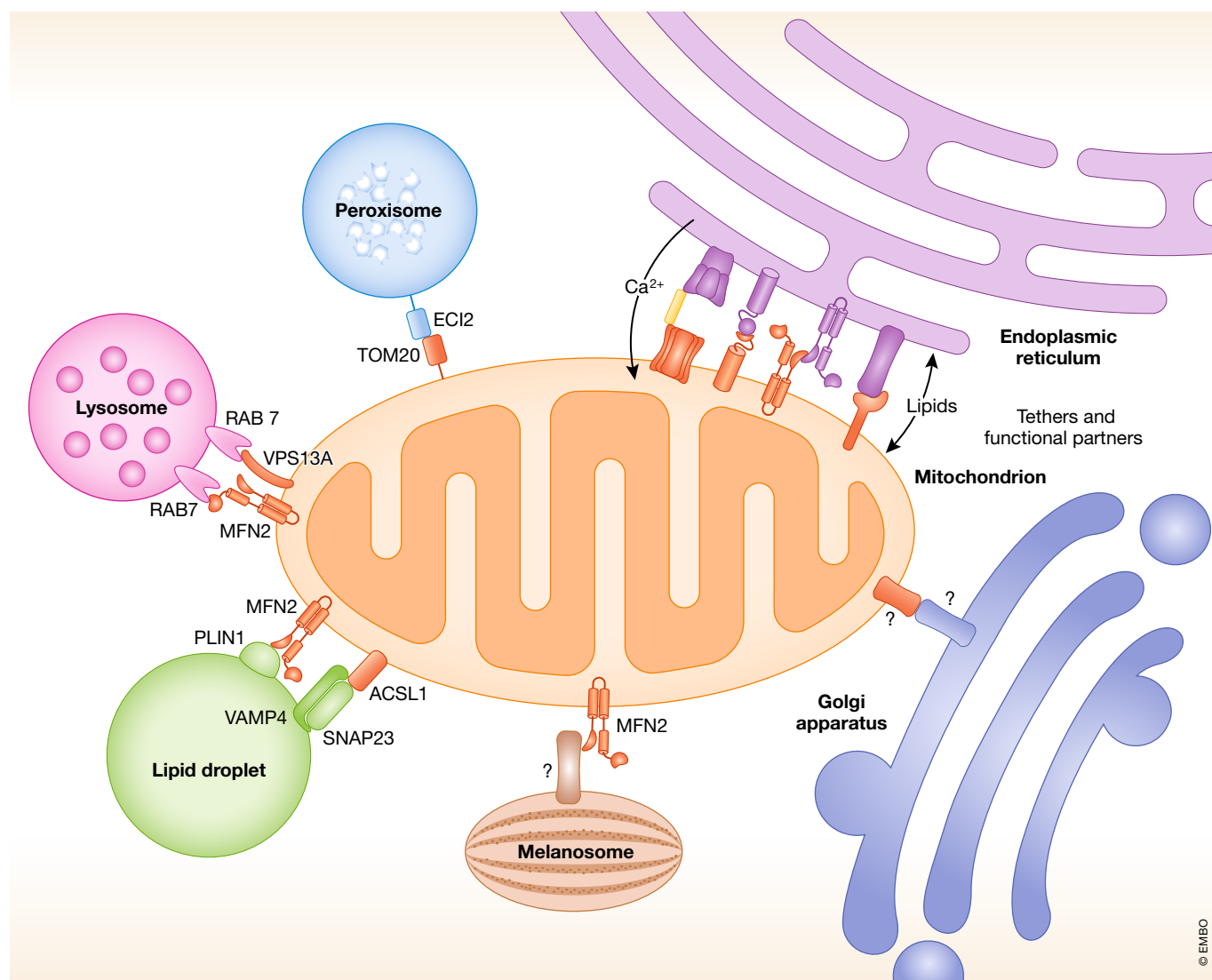


Figure 1. Contacts between mitochondria and other organelles.

Mitochondria interact with other membranous compartments in the cell. Mitochondria interact with the Golgi apparatus; however, the identities of the proteins involved in this interaction have not been discovered yet. Mitochondria are also in contact with lysosomes, but the mediators of these contacts remain unknown. MFN2 in mitochondria interacts with melanosomes. ECI2 and TOM20 bridge the peroxisome to the mitochondria. Mitochondria are anchored to lipid droplets by the MFN2–PLIN1 interaction. Mitochondria–ER contacts harbor a singular architecture and are hubs for several cellular processes such as Ca^{2+} signaling and lipid trafficking (see further details in Figs 2 and 3).

and FIS1 in mitochondria [11]; and MFN2 both in the ER and mitochondria [12]. These proteins not only shape mitochondria–ER contacts but also participate in the functions associated with these domains. PTP51 and VAPB are necessary to maintain Ca^{2+} transport between the ER and mitochondria [13]. Recently, MOSPD2 has

been proposed as a new tethering protein in the ER that interacts with PTP51 [14]. MOSPD2 is located at the contact sites of the ER with other organelles [14]. IP3Rs, GRP75, and VDAC1 form the gate through which Ca^{2+} leaves the ER and enters mitochondria [10]. These proteins are core components of a bigger complex specialized

in calcium channeling. Tethering capacity and calcium flux are sustained by the mitochondrial proteins PDK4 and TG2 [15]. The BAP31-FIS1 interaction is established at the MAM, upstream of apoptosis induction [11]. Moreover, this complex also participates in mitochondrial fission: FIS1 is a receptor for DRP1 in mitochondria, the major player in mitochondrial fission [16], and BAP31, once cleaved, is able to induce mitochondrial fission [17]. MFN2 is localized both in the mitochondria and in the ER, and in both cases, it is able to homooligomerize and to heterooligomerize with MFN1 to tether both organelles or to promote mitochondrial fusion [18,19]. Furthermore, the lack of MFN2 results in reduced mitochondrial Ca^{2+} uptake and in autophagosome formation arrest [12,20]. Although several studies argue that MFN2 is an organelle spacer [21,22], rather than a tether, we consider that the available data strongly support the role of MFN2 as a tether [12,23,24]. A recent study has suggested that another mitochondria-ER tethering complex could exist containing BiP in the ER membrane toward the ER lumen, WASF3 at the cytoplasm, and ATAD3A in the inner mitochondrial membrane (IMM) [25] (Fig 2). ATAD3A, WASF3, and BiP co-immunoprecipitate and silencing of *ATAD3A* downregulates BiP and WASF3 [25]. Given the location of these proteins in the cell, it is likely that they are part of a larger complex whose components remain undescribed.

Partial or total ablation of tethering proteins influences the architecture of mitochondria-ER contact sites. *GRP75* silencing decreases the interaction between IP3R1 and VDAC1 both in

HT22 mouse hippocampal neurons cells and in HuH7 human hepatocarcinoma cells [26,27]. This effect is also observed upon *MFN2* knockdown in HuH7 cells and H9c2 rat cardiomyoblasts [27,28]. *VDAC1* partial ablation diminishes the number of interaction spots between GRP75 and IP3R1 in HuH7 cells [27]. *IP3R1* silencing in hepatocytes does not alter the protein levels of the other IP3Rs [29]. *Pdk4* ablation in mice results in decreased MAM formation in skeletal muscle [15]. *Tg2* ablation in mouse embryonic fibroblasts (MEF) decreases the quantity of mitochondria-ER contact sites [30]. *Vapb* knockdown does not affect PTPIP51 expression or vice versa in NSC34 mouse motor neuron-like cells; however, it does reduce mitochondria-ER association [13]. In line with this, *Ptpip51* silencing in rat neonatal cardiomyocytes reduces mitochondria-ER contacts [31]. Moreover, the downregulation of *Vapb* or *Ptpip51* in NSC34 cells does not affect total MFN2 expression [13]. *MFN2* knockdown in human lung cancer H838 cells leads to an increase in ATAD3A localization to the MAM [32]. Both total and partial ablation of *Mfn2* in MEF cells increases the distance between the ER and mitochondria [23]. In agreement with this finding, in flexor digitorum brevis (FDB) muscles, mitochondria and ER apposition is reduced upon temporal *Mfn2* depletion [33]. It is likely that additional tethers or spacers will be identified in the future and that they will allow a more global view of the proteins involved in the maintenance of mitochondria-ER contacts. In addition, further studies are needed to determine whether the ablation of a single protein modifies the

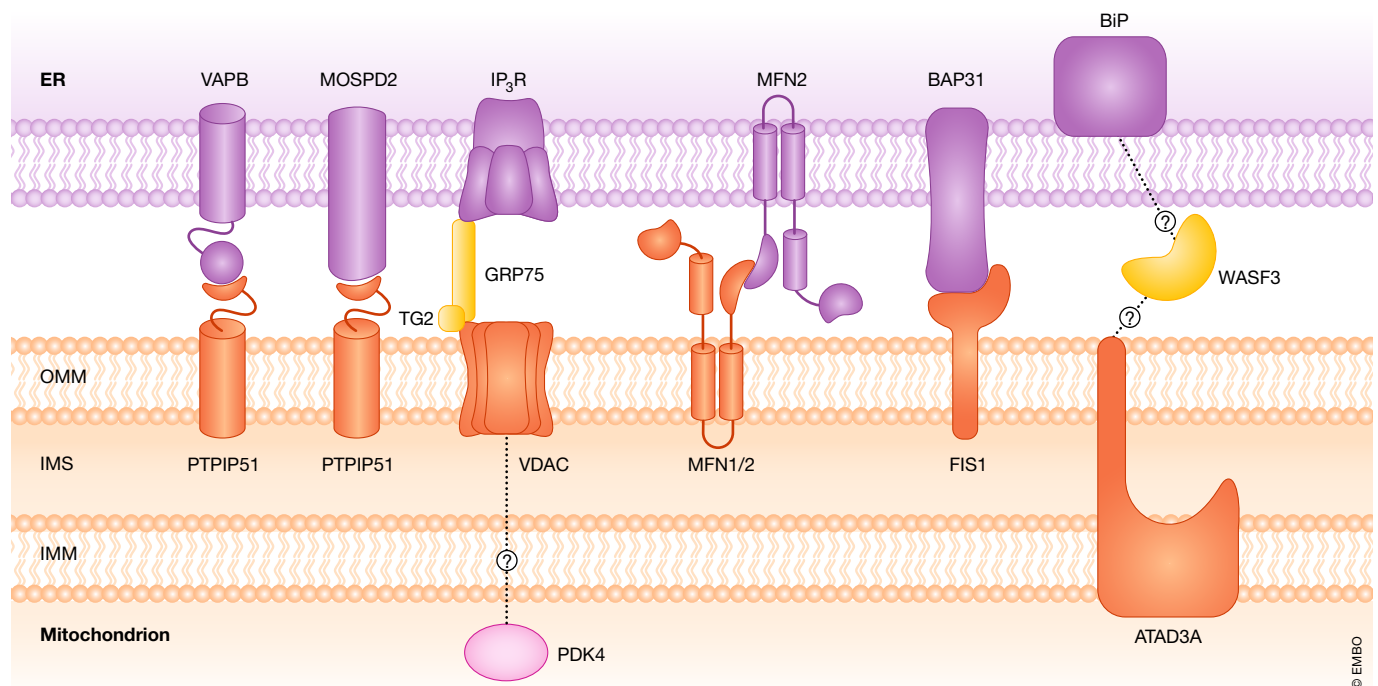


Figure 2. The architecture of mitochondria-ER contact sites: tethering complexes.

Mitochondria are bridged to the ER by several protein complexes. In the ER, VAPB or MOSPD2 bind to PTPIP51 in mitochondria. IP3R in the ER is anchored to VDAC in the OMM by the cytosolic protein GRP75. MFN2 is present both at the ER and in the OMM. From the ER, MFN2 interacts with either MFN1 or MFN2 in the mitochondria. BAP31 in the ER partners up with FIS1 in the mitochondria. BiP in the ER, WASF3 in the cytosol, and ATAD3A in the IMM have been suggested to form a complex that tethers both organelles.

expression of proteins or of genes involved in a different tether and to know whether these structures cooperate.

Functions linked to the mitochondria–ER contacts

The interface between ER and mitochondria harbors processes that are essential for the cell (Fig 3; Table 1). In this review, we have classified these processes in six groups: traffic of lipids, mitochondrial dynamics, Ca^{2+} signaling, ER stress, apoptosis initiation, and autophagosome formation.

Lipid trafficking

Intracellular lipid transport can occur by flip-flop from one side of a bilayer to the other, by vesicular trafficking, by lipid transfer proteins, or by diffusion within a bilayer [34]. MAMs are hubs for non-vesicular phospholipid and cholesterol transport, and this

process is linked to the synthesis of phospholipid and cholesterol intermediates. In this chapter, we analyze the progress in the traffic of lipids between ER and mitochondria and we highlight the remaining unexplored questions. Most of the advances so far have been obtained in cellular models, and *in vivo* assays would provide these findings with more robustness.

At the ER, phosphatidylcholine (PC) is converted into phosphatidylserine (PS) by PSS1 [35]. Mitochondria are not able to synthesize PS and therefore receive it from the ER [36,37]. The decarboxylation of PS in the mitochondria by PISD produces phosphatidylethanolamine (PE) [36,38]. This newly synthesized PE can then be translocated to the ER [37], where it is converted to PC by PEMT [39] or, less likely, to PS by PSS2 [35]. The discovery that newly synthesized PS and PE are transported between ER and mitochondria in a non-vesicular manner [37,40] was a key finding in the lipid trafficking field and an outstanding contribution to the understanding of the molecular biology of mitochondria and ER

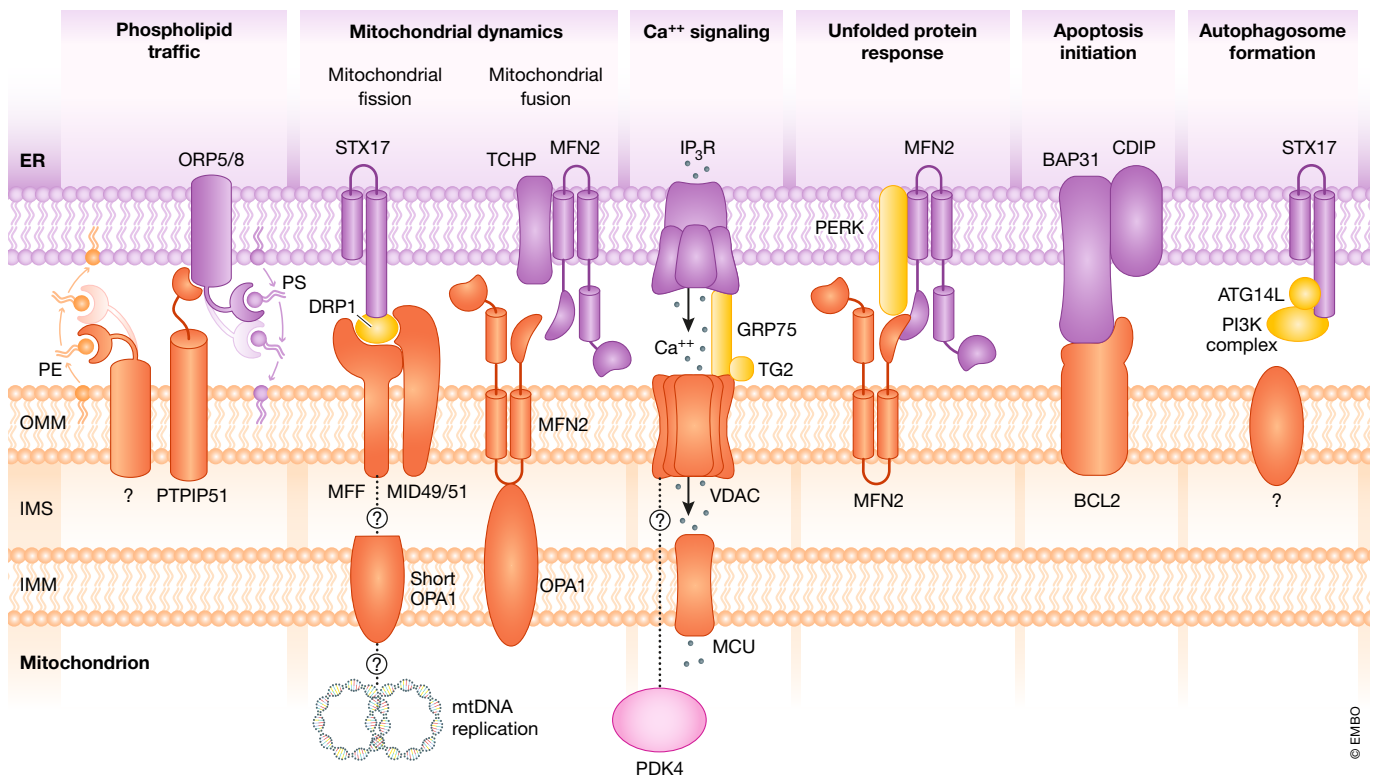


Figure 3. Cellular functions at mitochondria–ER contact sites.

The main processes that take place at the MAM are as follows: phospholipid trafficking, mitochondrial dynamics, Ca^{2+} signaling, unfolded protein response (UPR), apoptosis initiation, and autophagosome formation. MAMs are hubs for phospholipid exchange between the ER and mitochondria. Mitochondria take phosphatidylserine from the ER, which is supplied with phosphatidylethanolamine by mitochondria. Mitochondrial dynamics processes are regulated at the interface between the ER and mitochondria. The mitochondrial fission effector DRP1 is recruited by MFF and Mid49/51 to the mitochondrial surface, and it interacts with STX17 in the ER membrane. The ER wraps around the mitochondrion, which is finally excised into two daughter mitochondria after mtDNA replication. Mitochondrial fusion is promoted by TCHP binding to MFN2. This interaction separates MFN2 tethers and promotes the fusogenic function of mitochondrion-bound MFN2. The ER is the cellular Ca^{2+} reservoir. IP₃R, GRP75, and VDAC form a Ca^{2+} channeling complex that allows Ca^{2+} flux from the ER to mitochondria. MCU transports the intermembrane Ca^{2+} to the mitochondrial matrix. The UPR is regulated at the interface between mitochondria and the ER. One of the key regulators is MFN2, which inhibits the UPR by interacting with PERK. It is not known whether PERK interacts with MFN2 in mitochondria, MFN2 in the ER or with both. MAMs are also involved in the initiation of apoptosis. Sustained pro-apoptotic stimuli lead to BCL2 sequestration by the reticulum proteins BAP31 and CDIP in order to initiate apoptotic signaling cascades. Autophagosomes arise from mitochondria–ER contact sites. Proteins involved in autophagosome formation are recruited to these locations. STX17 in the ER attracts ATG14L and the PI3K complex. The mitochondrial component involved in this process is still not known.

Table 1. Mitochondria–ER contact sites proteins.

Protein	Location	Function in the MAM
ATAD3A	IMM	ER-mt tethering [25], lipid trafficking [52]
ATF6	ER	UPR [106]
ATG14	ER	Autophagosome formation [20]
BAK	OMM	Apoptosis [126]
BAP31	ER	ER-mt tethering [11], Apoptosis [11]
BAX	Cyt, OMM	Apoptosis [126]
BCL2	OMM	Apoptosis [126]
BiP	ER	ER-mt tethering [25]
CDIP1	ER	Apoptosis [126]
CypD	IMM	Apoptosis [125]
DRP1	OMM	Mitochondrial dynamics [252]
FIS1	OMM	ER-mt tethering [11], Mitochondrial dynamics [16], Apoptosis [11]
FUNDC1	OMM	Ca ²⁺ signaling [76], Mitochondrial dynamics [68]
GRP75	Mt	ER-mt tethering [10], Ca ²⁺ signaling [10]
INF2	ER	Mitochondrial dynamics [59]
IP3R	ER	ER-mt tethering [10], Ca ²⁺ signaling [10]
IRE1 α	ER	UPR [106]
MCU	IMM	Ca ²⁺ signaling [253]
MFF	OMM	Mitochondrial dynamics [62]
MFN1	OMM	ER-mt tethering [12], Mitochondrial dynamics [69]
MFN2	ER, OMM	ER-mt tethering [12], Mitochondrial dynamics [69], UPR [97]
MiD49	OMM	Mitochondrial dynamics [62]
MiD51	OMM	Mitochondrial dynamics [62]
ORP5	ER	Lipid trafficking [43]
ORP8	ER	Lipid trafficking [43]
PACS2	Cyt	ER-mt tethering maintenance [55]
PDZD8	ER	Lipid trafficking(?) [46]
PERK	ER	UPR [106]
PTPIP51	OMM	ER-mt tethering [9]
RyR	ER	Ca ²⁺ signaling [8]
SEC61	ER	Ca ²⁺ signaling [42]
SERCA1	ER	UPR [114]
STARD1	Cyt	Lipid trafficking [48]
STX17	ER	Autophagosome formation [20], Mitochondrial dynamics [65]
TSPO	OMM	Lipid trafficking [52]
VAPB	ER	ER-mt tethering [9]
VDAC1	OMM	ER-mt tethering [10], Ca ²⁺ signaling [10], Lipid trafficking [53]
WASF3	Cyt	ER-mt tethering [25]

apposition. It is not fully understood how PS is transported from the ER to mitochondria in mammalian cells; however, members of the oxysterol-binding protein (OSBP) family have been proposed to participate in this process. OSBP family proteins contain an OSBP-related ligand-binding domain that has the structure of a beta-barrel and binds PI4P and, in some cases, sterols [34]. Two members of this family, ORP5 and ORP8, localize at the ER

membrane facing the cytosol (Fig 3). ORP5 was first discovered to catalyze the exit of cholesterol from endosomes [41]. Later, it was found that ORP5 and ORP8 counter-exchange PS and phosphatidylinositol 4-phosphate (PI4P) between the ER and plasma membrane [42]. ORP5 and ORP8 are present at mitochondria–ER contact sites, where they interact with the tethering protein PTPIP51 [43] and could be responsible for PS transport to

mitochondria. In addition to the OSBP family, in yeast, the ERMES complex, which has no homology with any mammalian complex, tethers mitochondria to the ER and transfers PS from the ER to mitochondria [44]. Mmm1 and Mdm12, components of the ERMES complex, have been found to harbor an SMP domain that is responsible for phospholipid transfer [44,45]. This domain shows functional orthology with the SMP domain of mammalian proteins that localize at the ER, such as extended synaptotagmins and PDZD8 [45,46]. Expression of a chimeric form of Mmm1 containing the PDZD8 SMP domain in deficient *MMM1* yeast rescues mitochondrial defects. PDZD8 localizes at the ER fraction of MAMs [46]. The fact that PDZD8 harbors an SMP domain makes it a potential candidate for phospholipid exchange between the ER and mitochondria.

Sterols, oxysterol, and bile acids are synthesized in mitochondria. These molecules originate from cholesterol that is imported into mitochondria from several sources: ER, LD, and endosomes (reviewed by Elustondo *et al* [47]). Here, we focus on cholesterol transport from the ER, which is performed by STARD1 [48]. STARD1 contains a lipid binding domain known as START, which particularly in this protein has specificity for sterols [49,50]. In mitochondria-ER contact sites, STARD1 is recruited to the OMM where it forms a complex with the OMM proteins TOM22 and VDAC2 and the ER proteins BiP, ERLIN2, and SLC [48]. STARD1 incorporates ER-cholesterol into the OMM so that it can be transported to the IMM, where CYP11A1 further processes it [51]. The complex that moves cholesterol from the OMM to the IMM is formed by VDAC1 and TSPO in the OMM and by ATAD3A and CYP11A1 in the IMM [52]. STARD1 interacts with members of this complex, namely VDAC1 and TSPO [53], thus linking cholesterol incorporation from the ER to its processing in the mitochondrial matrix.

The modification of proteins involved in lipid trafficking in the MAM influences other protein complexes and functions that take place at the MAM, and it also affects the interaction between mitochondria and the ER. Moreover, the alteration of tethering proteins has an impact on lipid transport between the two organelles. *ORP5* and *ORP8* depletion from HeLa cells alters mitochondrial morphology and respiration; however, the number of mitochondria-ER contact sites is not affected [43]. Overexpression of *ORP5* and *ORP8* increases mitochondrial Ca^{2+} concentration in HeLa cells after histamine treatment, although depletion of these proteins does not alter Ca^{2+} signaling [54]. Also, when the tethering protein PTPIP51 is overexpressed in HeLa cells, the presence of *ORP5/8* at mitochondria-ER contact sites is increased [43]. However, it has not been assessed whether PS transport is increased upon PTPIP51 overexpression. Depletion of *PDZD8* leads to reduced contact surface between the ER and mitochondria and to reduced Ca^{2+} flux into mitochondria in HeLa cells [46]. The expression of a loss-of-function mutant of *PACS2*, a cytosolic protein involved in tether maintenance, in A7 human skin melanoma cells diminishes the levels of *PSS1* and *FACL4*, a fatty acid metabolism enzyme [55]. Regarding cholesterol trafficking proteins, *TSPO* downregulation is observed upon the deletion of the tethering protein *VDAC1* in U87 MG human glioma cells [56]. Furthermore, *TSPO* was demonstrated to inhibit mitochondrial Ca^{2+} uptake by promoting *VDAC1* phosphorylation [57]. The available evidence for the role of different proteins in lipid trafficking is limited to cultured cells, and further studies should be done to validate their function in the context of the whole animal.

Mitochondrial dynamics

Mitochondria change their morphology in order to efficiently adapt to the energetic demands of the cell, to respond to stress conditions (such as nutrient deprivation), or to react to apoptotic stimuli. Mitochondria-ER contacts are crucial for mitochondrial fission, since ER tubules surround and constrict mitochondria at the sites of division [58]. This constriction is mediated by actin filaments that accumulate between mitochondria and the ER and that are polymerized at the ER membrane by INF2 [59]. INF2-mediated actin polymerization leads to an accumulation of myosin type II [60], an increase in mitochondria-ER contacts, and the subsequent stimulation of mitochondrial Ca^{2+} uptake before constriction of the IMM and mitochondrial division [61]. The main driver of mitochondrial fission is the dynamin-related GTPase *DRP1*, which moves from the cytosol to the OMM, where it interacts with membrane proteins such as *FIS1*, *MFF*, *MiD49*, and *MiD51* [62]. *MFF*, *MiD49*, and *MiD51* recruit *DRP1* at the mitochondrial surface to form trimeric complexes in which *MiD49/51* compete with *MFF* for *DRP1* interaction [63]. *DRP1* activity can be regulated by redox signals. *PDIA1* modifies *DRP1* to negatively regulate its activity and to maintain mitochondrial reactive oxygen species (ROS) at low levels [64]. Conversely, an increase in mitochondrial ROS results in oxidation of *DRP1* and in increased mitochondrial fission which favors mitochondrial ROS accumulation [64]. However, further insight is necessary for a deep characterization of how redox states of cells influence mitochondrial dynamics. At mitochondria-ER contact sites, the ER protein *STX17* interacts with mitochondria-bound *DRP1* to support fission [65] (Fig 3). Under starvation conditions, *STX17* releases *DRP1* to initiate autophagosome formation and to promote the elongation of mitochondria to be protected from autophagy [65,66]. Recent findings have revealed that mitochondria-ER contacts are sites for mitochondrial DNA (mtDNA) synthesis and that nascent mtDNA stays in the daughter mitochondria after fission [67]. How the mitochondrial fission machinery is coupled to mtDNA replication has not been explained to date. Mitochondrial fission is a process coupled to mitochondrial removal by mitophagy. The link between these two processes is the OMM protein *FUNDC1*, which localizes at mitochondria-ER contact sites and interacts with calnexin in the ER and *DRP1* on the mitochondrial surface [68]. *FUNDC1* promotes both autophagosome recruitment and mitochondrial fission [68].

Furthermore, the interaction between the ER and mitochondria is a key player in the regulation of mitochondrial fusion. This process occurs first by fusion of the OMMs, followed by fusion of the IMM [69]. The key players in these two processes are the dynamin-like GTPases *MFN1* and *MFN2* in the OMM and *OPA1* in the IMM [69]. Mitofusins present in mitochondria interact with each other to fuse the OMMs. After OMM fusion, *OPA1* oligomerizes and IMM fuse. A cleaved isoform of *OPA1* is associated with mitochondrial fission rather than fusion [70]. It is still not clear how many *MFN1*, *MFN2*, and *OPA1* molecules oligomerize to carry out this function. Dimeric and tetrameric interaction models have been proposed [71–73]. As mentioned before, *MFN2* is present at both sides of the MAM, and it participates in mitochondria-ER tethering complexes [74]. These two roles of *MFN2* are mutually exclusive and determined by its interaction with *TCHP* (Fig 3). *TCHP*, a MAM protein localized at the ER, prevents mitochondria-ER tethering and favors mitochondrial elongation when it is bound to *MFN2* [74].

The alteration of mitochondrial dynamics proteins has an impact on MAM functions. Moreover, changes in certain tethering proteins alter mitochondrial morphology. Regarding the mitochondrial fission machinery, the induction of INF2-mediated actin polymerization with ionomycin in U2OS human osteosarcoma cells leads to an increase in mitochondrial Ca^{2+} and mitochondria–ER contact sites [61]. Moreover, the chemical inhibition of DRP1 in PC12 rat pheochromocytoma cells leads to a reduction in ER Ca^{2+} release compared to untreated cells and concomitantly decreases mitochondrial Ca^{2+} intake [75]. *Fundc1* overexpression in mouse cardiomyocytes increases Ca^{2+} release from the ER to mitochondria [76]. The role of FUNDC1 in Ca^{2+} release will be further assessed in this review. Concerning mitochondrial fusogenic proteins, the lack of MFN1 and MFN2 produces an aberrant distribution of pro-apoptotic proteins in the OMM, thus reducing apoptotic signaling [77]. *Mfn2* ablation in mouse hearts increases the levels of the anti-apoptotic protein BCL2 [78]. Loss of function of the tethering protein VAPB in *Caenorhabditis elegans* impairs mitochondrial dynamics [79], although this has not been reported in mammals to date. The depletion of the tether maintainer PACS2 in A7 cells results in mitochondrial fragmentation and uncoupling from the ER [55].

Ca^{2+} signaling

Before MAMs were studied at the molecular level, there was evidence that regions of mitochondria in close proximity to the ER participated in Ca^{2+} signaling [80]. The ER lumen is the cell Ca^{2+} storage area and the sites of proximity of the ER to mitochondria harbor high Ca^{2+} microdomains. The ER incorporates Ca^{2+} from the cytoplasm by SERCA1/2/3 ATPases [81,82]. ATP is hydrolyzed by SERCA transporters in order to allow Ca^{2+} entry to the ER lumen [81]. Ca^{2+} is released from the ER by the IP3R1/2/3 and the ryanodine receptors (RyR1/2/3), transferred to the mitochondrial intermembrane space by VDAC porins, and finally introduced into the mitochondrial matrix by the mitochondrial Ca^{2+} uniporter (MCU) complex (reviewed by Giorgi *et al* [83]). Ca^{2+} transport at the MAMs is depicted in Fig 3. In the OMM, TOM70 recruits IP3R to favor Ca^{2+} transference to mitochondria [84] and, in the cytosolic part of the MAM, GRP75 couples IP3Rs to VDAC [10], thereby allowing rapid Ca^{2+} flux into mitochondria. CypD, a protein involved in apoptosis initiation and in mitochondrial ATP synthase modulation [85], interacts with and maintains the VDAC1-GRP75-IP3R1 complex [28]. Another Ca^{2+} channel in the ER is the SEC61 complex, a translocon at the ER from which Ca^{2+} leaks passively to the cytosol [86,87], and once in the cytosol, it can be sequestered into mitochondria by VDAC. Ca^{2+} import to mitochondria stimulates the translocation of cristae accumulated H_2O_2 to MAMs, which results in the appearance of redox nanodomains at the mitochondria–ER interface which enhance Ca^{2+} efflux from the ER [88]. The accumulations of ROS at the MAMs arise as a consequence of active Ca^{2+} exit from the ER and do not occur with passive Ca^{2+} leakage. Mitochondrial ROS can regulate as well Ca^{2+} flux to the mitochondrial matrix by MCU oxidation, which increases the MCU oligomerization and thus its activity [89]. Insulin signaling modulates IP3R Ca^{2+} flux to mitochondria via mTORC2. After insulin stimuli, mTORC2 in the MAM phosphorylates AKT [90], which in turn phosphorylates IP3Rs to reduce Ca^{2+} release from the ER [91,92]. BiP limits ER Ca^{2+} leakage through the Sec61 complex by binding to the ER luminal region of Sec61 α [93].

Alterations in Ca^{2+} trafficking between the ER and mitochondria affect mitochondrial morphology. Mitochondria of brown adipose tissue (BAT) of mice fed on Ca^{2+} excess for 3 days are larger and fewer than in control mice [94]. MFN1 and MFN2 are increased in the BAT of these mice, whereas DRP1 is decreased [94]. Mitochondria–ER contacts are also increased in BAT after Ca^{2+} treatment [94]. Moreover, MCU ablation in U2OS cells prevents mitochondrial division [61]. In addition to its role in mitochondrial dynamics, FUNDC1 interacts with the ER Ca^{2+} channel IP3R2 and promotes Ca^{2+} flux to mitochondria [76]. The depletion of *Fundc1* in mouse cardiomyocytes and H9c2 myoblasts leads to a decrease in IP3R2 and colocalization between mitochondria and the ER [76]. The authors of this study proposed that FUNDC1 and IP3R2 act together as a tethering complex of mitochondria and the ER. FUNDC1 ablation also decreases the levels of the MAM maintenance protein PACS2 [76]. Inhibition of ER Ca^{2+} uptake by SERCA initiates UPR and eventually provokes apoptosis [95]. PDK4 inhibition decreases Ca^{2+} flux in C2C12 myoblasts [15]. *Tg2* ablation impairs Ca^{2+} flux in MEF [30]. The alteration of mitochondria–ER tethers also has an impact on Ca^{2+} trafficking [76]. Disruption of PTPIP51 and VAPB tethering complex impairs Ca^{2+} homeostasis in HEK293 cells [9]. The knock-down of either *VAPB* or *PTPIP51* decreases Ca^{2+} uptake into mitochondria [9], and overexpression of these proteins increases Ca^{2+} flux to mitochondria [96]. *MFN2* depletion has been reported to cause both increase and decrease in Ca^{2+} uptake [33,97]. In FDB muscles, mitochondrial Ca^{2+} uptake decreased upon temporal *Mfn2* depletion [33]. However, the protein levels of Ca^{2+} transport proteins (MCU, SERCA1, RyR1) remained unchanged [33]. In contrast to this result, *Mfn2* depletion in MEF cells caused Ca^{2+} overload in mitochondria [97].

ER stress

When protein folding efficiency is disturbed at the ER, misfolded proteins accumulate in the lumen and cause ER stress. This can happen as a result of certain conditions, such as nutrient deprivation, hypoxia, loss of Ca^{2+} homeostasis, free fatty acids, and GM1 ganglioside accumulation [98–103]. Why stress conditions lead to protein misfolding remains unknown. The accumulation of large amounts of these misfolded proteins activates the unfolded protein response (UPR) in order to restore protein homeostasis or to induce apoptosis [104,105]. The UPR has three main branches, which are interconnected after the signal transducers in the ER, namely PERK, ATF6, and IRE1 α , have been stimulated [106]. What is known about UPR branches has been discovered by treating cells and animals with exogenous compounds or unphysiological harvesting conditions to provoke protein misfolding; nevertheless, the natural cause of protein folding defects and their accumulation is not known. The activation of PERK induces eIF2 α phosphorylation. Phosphorylated eIF2 α inhibits global protein translation and activates ATF4, which translocates to the nucleus to induce the expression of survival genes [107]. Prolonged UPR activation induces apoptosis through the activation of CHOP by ATF4 [108]. The ATF6 branch of the UPR starts with the translocation of ATF6 from the ER to the Golgi apparatus for cleavage [109]. Cleaved ATF6 is a transcription factor that induces ER-associated degradation genes [110] and XBP1 [111]. IRE1 α activation induces splicing of XBP1 mRNA to enhance cell survival [111], activation of MAPK [112] to modulate autophagy and apoptosis, and IRE1 α -dependent mRNA decay [113]. ER stress

signaling can be amplified at MAMs by SERCA1 truncated isoform (ER), which acts upstream of the PERK-eIF2 α -ATF4-CHOP pathway [114]. Moreover, the location of PERK at MAMs contributes to the maintenance of mitochondria-ER contact sites and to the enhancement of ROS-mediated mitochondrial apoptosis signaling [115]. UPR mission is to restore cellular homeostasis by correcting protein folding and recovering damaged ER environment [116]. As long as protein folding efficiency is not resolved, UPR is activated [116]. ER stress results in increased mitochondria coupling to ER, which increases ATP production, oxygen consumption, and mitochondrial Ca²⁺ uptake [117]. Chronic UPR signaling initiates a signaling cascade in the MAM that eventually leads to apoptosis [116]. This signaling pathway is discussed in the following section.

The alteration of ER stress proteins, especially the IRE1 α branch, impairs lipid handling. The hepatic depletion of *Xbp1* in mice decreases circulating levels of fatty acids, triglycerides, and sterols, compared to control mice [118]. Lack of XBP1 in the liver impairs cholesterol processing for the generation of bile acids in these mice [119]. This phenotype is recovered by overfeeding the mice with cholesterol [119]. A separate study using liver *Xbp1* knockout mice also reports decreased plasma levels of cholesterol and triglycerides compared to control mice [120]. This effect is prevented by knocking down IRE1 α [120]. The modification of mitochondria-ER tethering proteins leads to ER stress. MFN2 interacts with PERK and represses its activity [97]. MFN2 loss of function in MEF cells dysregulates the three branches of the UPR by enhancing the PERK-eIF2 α -ATF4-CHOP pathway [97]. Ablation of *Mfn2* results in the continuous activation of PERK, and PERK silencing in these cells causes ROS production, the restoration of mitochondrial Ca²⁺ levels, and an improvement of mitochondrial morphology [97]. However, it is not known whether PERK interacts with mitochondrial MFN2, ER MFN2, or both (Fig 3). The increase in mitochondria coupling to ER upon ER stress [117] is coherent with the upregulation of MFN2 expression observed in MEFs upon ER-stress induction with thapsigargin and tunicamycin [121]. In the same study, the authors show that ablation of *Mfn2* in MEFs upregulates ER stress markers (BiP, GRP94, and ATF4) [121]. Specific ablation of *Mfn2* in mouse cardiac myocytes also causes an increase in the expression of BiP, GRP94, and ATF4 [121]. Another tethering protein, VAPB, represses the UPR by binding to ATF6 [122]. Overexpression of *VAPB* both in HEK293 and NSC34 cells decreases ATF6/XBP1-induced luciferase activity upon tunicamycin stimulation, even in combination with *ATF6* overexpression [122].

Apoptosis initiation and ER stress-mediated apoptosis

When cells cannot adequately handle certain stress stimuli, they activate pathways that lead to cell death. A complex formed by BAP31 and FIS1 at mitochondria-ER contact sites is able to transfer apoptotic signals back and forth from the mitochondria to the ER [11]. In response to apoptotic stimulus, the FIS1-BAP31 complex recruits procaspase-8 to be activated [11]. Active caspase 8 cleaves BAP31 into a pro-apoptotic form that, together with FIS1, promotes Ca²⁺ release from the ER [11,123] and mitochondrial fission [17]. Mitochondrial Ca²⁺ increase leads to CYPD activation in the IMM to open the permeability transition pore from which molecules that drive apoptosis are released [124,125]. Under sustained ER stress conditions, CDIP and BAP31 interact at the ER side of the MAM to

sequester the anti-apoptotic factor BCL2 located at the OMM, in order to promote apoptosis (Fig 3) [126]. The protein PACS2, which localizes in MAMs, has been reported to promote the translocation of the pro-apoptotic protein BID to mitochondria [55]. The CDIP1-BAP31-BCL2 complex, together with the truncated form of Bid and caspase-8 activation, promotes BAX and BAK oligomerization [126]. BAX translocates from the cytosol to the OMM, where BAK locates constitutively. The activation of these two molecules occurs after their oligomerization [127]. Although not yet demonstrated, it is believed that cytochrome *c* exits mitochondria from the pores formed by these oligomers [128]. After cytochrome *c* release, an apoptotic protease cascade is initiated [129].

Since MAMs are hubs for apoptosis initiation and this process involves Ca²⁺ signaling at the MAM and mitochondrial fission, the alteration of some apoptosis initiators has an impact on these MAM functions. *BCL2* loss-of-function mutations in Jurkat T cells decreases mitochondrial Ca²⁺ uptake [130]. When *Bak* is knocked out in MEF cells, mitochondria are not fragmented in response to apoptotic stimulus [131]. Overexpression of *Bax* promotes MFN2-mediated mitochondrial fusion in MEFs [132]. It has been proposed that BAX plays a dual role: The soluble cytoplasmic form promotes mitochondrial fusion and, when activated and recruited to the OMM, it participates in apoptosis [132].

Autophagosome formation

In order to preserve cellular homeostasis, damaged or unnecessary components of the cell must be degraded or recycled. This process is achieved by autophagy. Autophagosomes engulf damaged or needless components and can originate from ER-mitochondria contact sites [20]. The ER side of the MAM region, where proteins related to autophagosome formation start to accumulate, is known as the isolation membrane. This structure protrudes from the ER and finally closes around the cellular components to be eliminated, forming a vesicle named the autophagosome [133]. After starvation stimulus, ATG14 is recruited to the MAM by STX17 [20]. This results in accumulation of the components of the class III PI3K complex (ATG14, BECN1, VPS34, and VPS15) at the MAM [20] (Fig 3) and contributes to the initiation and nucleation of the isolation membrane. Next, the ATG16L1 complex (ATG5-ATG12-ATG16L) is recruited to the isolation membrane, where it binds PE to LC3 [134]. Lipidated LC3 molecules associate with the isolation membrane and remain attached once the autophagosome is closed [133]. How the isolation membrane closes is still poorly understood.

Alterations in tethering proteins have an impact on autophagosome formation. The absence of MFN2 or PACS2 at the MAM impedes STX17-mediated ATG14 recruitment to this area in HeLa cells [20]. MFN2 and PACS2 seem to be crucial for autophagosome biogenesis; nevertheless, their role in this process has not been described yet. Moreover, the tightening of mitochondria-ER contact sites by overexpression of *VAPB* and *PTPIP51* results in decreased autophagosome formation after torin-1 or rapamycin stimulus in HeLa and HEK293T cells [135]. Conversely, the opposite effect is observed when *PTPIP51* and *VAPB* are ablated in HeLa and HEK293T cells [135]. Future work will unravel what is the precise role of the MAM in autophagosome formation and which MAM proteins recruit the autophagosome biogenesis machinery. Moreover, since membrane contact sites from other

organelles have also been proposed as autophagosome factories [20,136–138], a remaining open question in the field is whether autophagosomal content to be degraded is influenced by the origin of the autophagosome.

Consequences of metabolic challenge in mitochondria–ER contacts

Human, animal, and cellular studies have revealed that metabolic alterations can perturb mitochondria–ER contact sites. In this section, we review the observations that document the impact of altered metabolic homeostasis on the architecture and functioning of MAMs, and also the impact of nutrient availability and lysosomal storage disorders.

The impact of metabolic disorders on the architecture and functioning of mitochondria–ER contacts

Some studies have reported alterations in mitochondria–ER contacts in liver and in muscle cells upon metabolic dysregulation. Surprisingly, there is considerable discrepancy in the data available. Thus, liver analysis of ob/ob obese mice and mice subjected to a high-fat diet (HFD) showed an increased abundance of MFN2, IP3R, and PACS2 in MAM fractions, in parallel to increased mitochondria–ER contacts, and an excess of mitochondrial Ca^{2+} accumulation [29]. Moreover, a forced increase in the mitochondria–ER contacts, induced by expression of an artificial linker in livers from control mice, caused an increased mitochondrial Ca^{2+} uptake and impaired glucose homeostasis [29]. Conversely, *Ip3r1* knockdown in obese mice caused a reduced Ca^{2+} flux, and similarly, *Pacs2* knockdown led to a decreased physical interaction between the ER and mitochondria, and to improved glucose homeostasis [29].

In contrast to the results obtained by Arruda *et al*, Tubbs *et al* [27] detected that mitochondria–ER contacts (measured by quantifying VDAC1–IP3R1 interaction) were decreased in hepatocytes isolated from mice subjected to diet-induced diabetes and from ob/ob mice. Moreover, the overexpression of *CypD* in these hepatocytes increased mitochondria–ER contacts and improved the effects of insulin. A third study revealed that HepG2 hepatoma cells treated with palmitate showed reduced mitochondrial Ca^{2+} flux, lower mitochondria–ER contacts, and impaired insulin sensitivity [139]. Under these conditions, *Mfn2* overexpression ameliorated the mitochondria–ER contact area and insulin sensitivity. We do not yet know whether the opposite observations are a consequence of differences in the methodology used (proximity ligation assays or transmission electron microscopy, or tissue sections versus isolated hepatocytes), or whether they are based on subtle differences in the nutritional state of the animals studied. Regarding the impact of metabolic alterations in liver ER stress and ER Ca^{2+} homeostasis, the main studies of the field show more consensus. Livers of obese mice show increased ER stress [140,141] and reduced cellular SERCA2b levels [140] or impaired SERCA activity in the ER [141]. Glucose tolerance was increased and ER stress was alleviated in obese and diabetic mice by liver exogenous expression of SERCA2b [140,141].

In the skeletal muscle of ob/ob mice or in mice subjected to a high-fat, high-sucrose diet, Tubbs *et al* found impaired insulin

signaling and decreased levels of MAM proteins, accompanied by a decrease in mitochondria–ER contacts (measured by quantifying VDAC1–IP3R1 interaction). In human myotubes from healthy patients, mitochondria–ER contacts were also diminished after palmitate treatment [142]. Mitochondrial Ca^{2+} concentration was somewhat decreased compared to untreated cells. *Mfn2* or *Grp75* overexpression reversed the effects of palmitate on MAM proteins and on insulin signaling [142]. Moreover, myotubes from obese patients and from obese patients with type 2 diabetes showed decreased mitochondria–ER contacts compared to those of healthy patients [142]. In contrast to these results, Arruda *et al* [29] found an increase in the MAM proteins MCU and RyR in soleus muscles from ob/ob and HFD-fed mice, suggesting an enrichment in MAMs under these conditions. In line with these results, Thoudam *et al* [15] found increased levels of IP3R1, VDAC1, and GRP75 in the MAM fraction of skeletal muscle of HFD-fed mice and ob/ob mice. Furthermore, they observed increased levels of MFN2 in HFD-fed mice. Moreover, using proximity ligation assays, they detected increased IP3R1–GRP75–VDAC1 interactions in HFD-fed mice and ob/ob mice [15]. Transmission electron microscopy of muscle MAM surface revealed increased MAM area in HFD-fed mice compared to animals on a chow diet [15]. Interestingly, the authors quantified the distance between juxtaposed ER and mitochondria and found that in HFD-fed mice the proportion of loose contacts between the ER and mitochondria was increased. As mentioned in the liver studies, we do not know whether the differing observations detected in muscles of obese mice are due to differences in the methodology used or to differences in the nutritional state of the animals studied. In any case, further studies are required to clarify the nature and kinetics of the changes that occur in mitochondria–ER contacts during metabolic dysregulation in muscle and in liver.

Insulin-resistant conditions such as obesity and type 2 diabetes are characterized by altered muscle expression of MFN2, which may participate in the alterations in mitochondria–ER contacts. Thus, *Mfn2* is repressed in the muscles of obese Zucker rats [143]. Obesity induced by a HFD during 40 weeks also reduces MFN2 and MFN1 expression in muscle [144]. In addition, the muscles of obese subjects also show a reduced expression of MFN2 compared with lean subjects [143,145]. In contrast, bariatric surgery-induced body weight loss was reported to increase *MFN2* gene expression in the skeletal muscle of morbidly obese subjects [146–148] in parallel with increased insulin sensitivity [146–148]. Type 2 diabetic patients also show reduced MFN2 expression in the skeletal muscle compared with control subjects [145,149], and this occurs both in obese and non-obese type 2 diabetic patients [145]. The dysregulation of *MFN2* is unlikely to be a consequence of reduced insulin action because the expression of this gene in lean, obese, or type 2 diabetic subjects is not altered in response to 3 h of hyperinsulinemia during clamp studies. Neither is the expression of this protein affected when cultured muscle cells are chronically incubated in the presence of insulin [145,150]. Induced insulin resistance in rats by high sucrose diet provokes slower contraction and elongation of cardiomyocytes [151]. ER Ca^{2+} uptake by SERCA is impaired in these cardiomyocytes although the levels of this protein remain unchanged [151].

Studies in beta-cells also indicate the existence of alterations in response to metabolic stress. Thivolet *et al* [152] reported an

increased IP3R2 and decreased VDAC1 expression, accompanied by reduced mitochondria–ER contact sites in beta-cells from type 2 diabetic patients. In addition, Min6-B1 beta-cells exposed to palmitate show ER stress, reduced mitochondria–ER contacts, and impaired insulin secretion [152]. Zhang *et al* [153] reported increased VDAC1 abundance accompanied by mislocalization of part of VDAC1 to the plasma membrane. INS1E beta-cells also respond to elevated glucose concentrations in the culture medium by upregulating VDAC1 [154]. High glucose environment increases *Bax* mRNA levels and stimulates BAX-dependent apoptosis in mouse islets [155].

POMC neurons respond to a HFD by reducing the number of mitochondria–ER contacts compared to mice on a regular diet [156]. Under these conditions, MFN2 levels are reduced in HFD mice [156]. In HFD-fed mice, stimulation of DRP1-dependent mitochondrial fission in the dorsal vagal complex induces ER stress and insulin resistance [157], and inhibition of DRP1 restores ER stress, insulin resistance, and hepatic glucose metabolism.

An increase in mitochondria–ER contacts, increased expression of IP3R1, IP3R2, and PACS2 protein levels, and greater mitochondrial Ca^{2+} uptake and apoptosis has been documented in oocytes from HFD-treated mice [158]. These changes compromise oocyte maturation.

In conclusion, available data suggest that metabolic stress linked to insulin resistance, obesity, or type 2 diabetes affects mitochondria–ER contacts, and may occur in various cells or tissues. Liver and muscle have been deeply analyzed in this context, and the observations annotated by the authors differ across the studies that we have discussed. Whether the consequence of this metabolic stress in liver and muscle is to increase or to reduce the surface of contact between the ER and the mitochondria is still under debate. Moreover, current data regarding the expression levels of the tethering proteins MFN2, IP3R, VDAC, and GRP75 under conditions of insulin resistance, obesity, or type 2 diabetes annotated across several studies are not uniform. As a consequence, the functional impact of the modification of these contacts is not known. An example that illustrates this lack of consensus is the persistent discrepancy on the observations regarding Ca^{2+} influx into mitochondria under metabolic stress conditions. In order to solve this puzzle, there is need of a precise characterization of the molecular mechanisms involved in the response to metabolic stress as well as the establishment of standard procedures to perform this characterization.

The adaptation of mitochondria–ER contact sites to nutrient availability

Mitochondria–ER contact sites respond to changes in nutrient availability by modifying Ca^{2+} signaling, initiating autophagy or activating the UPR. The first evidence for this response was observed by Sood *et al* [159] in postprandial mouse livers. Five hours postprandial livers showed larger mitochondria–ER contact sites than 2 h postprandial livers. In agreement with this study, livers of fed mice show reduced mitochondria–ER contacts compared to those of overnight fasted mice, and this occurs without a significant modification of the ER or mitochondrial content [160]. The interactions between VDAC1 and IP3R1 are reduced in fed compared to fasted mice. VDAC1 and GRP75 are also decreased upon feeding in mouse liver, whereas IP3R1 protein expression remains unchanged [160]. In a different study, mice

refed after 22 h of fasting showed a 50% decrease in hepatic IP3R1 levels compared to fasted animals [161]. Interestingly, primary hepatocytes cultured in the presence of high glucose (17 mM) also show a reduced VDAC1–IP3R1 interaction compared to cells cultured in the presence of 5 mM glucose. In conclusion, these data suggest that glucose availability is a key signal in the regulation of mitochondria–ER contacts in liver cells.

Genetic obesity appears to alter the dynamics of mitochondria–ER contacts. Thus, the livers of obese ob/ob mice do not reproduce the mitochondria–ER uncoupling during fed to fasted transition. MAMs are reduced in fasting conditions in ob/ob compared to lean mice, and no differences are detectable compared to obese mice analyzed during fed conditions [160]. Moreover, the interaction between IP3R1 and VDAC1 is reduced in fasted ob/ob mice compared to lean mice and no significant differences are observed in ob/ob mice when comparing fed and fasted states [160]. In keeping with these data, ob/ob hepatocytes cultured in the presence of high glucose do not show a reduced VDAC1–IP3R1 interaction compared to cells cultured in the presence of 5 mM glucose, again indicating that obesity disrupts glucose-induced control over mitochondria–ER contacts.

Nutrient deprivation causes the inhibition of mTOR activity, which activates autophagy [162] and promotes the formation of autophagosomes. In this regard, autophagosomes originate at mitochondria–ER contact sites [20], and the disruption of MAMs by depletion of *Mfn2* or *Pacs2* results in impaired autophagosome formation [20,163]. Moreover, glucose and amino acid deprivation causes mitochondrial elongation [66], which occurs through inhibition of DRP1 and activation of MFN1, thus protecting mitochondria against autophagic degradation. In all, available data allow us to propose that the modulation of mitochondria–ER contact sites is linked to the modulation of autophagosome formation and mitochondrial morphology through mechanisms that require extensive research efforts. It is likely that signals such as mTOR, and ER stress response, which are modulated by nutrient availability [164,165], participate in mitochondria–ER contacts during fed to fasted transitions.

In summary, ER and mitochondria contact surface increases in response to lack of nutrients. This adaptive increase in contact sites is impaired under obesogenic conditions. However, it is still uncertain whether these changes in the MAM are accompanied by a modification in the expression levels of tethering proteins. Enhanced autophagosome formation and ER-stress response are probably the functional consequences of MAM enlargement.

Metabolic impact of alterations in proteins participating in mitochondria–ER contacts

The concept that metabolic homeostasis is determined by modulation of mitochondria–ER contact sites arose after several reports documenting that *Mfn2* deficiency disrupts metabolism in cells and in animal models [97,156,166,167]. In addition, the metabolic effects caused by *Mfn2* deficiency differ to those detected upon *Mfn1* ablation, thereby indicating that they are probably due to compromised mitochondria–ER contacts rather than to impaired mitochondrial fusion. Subsequent mouse studies have revealed that ablation of proteins participating in mitochondria–ER contacts

causes three distinct phenotypes, namely (i) reduced glucose tolerance and insulin signaling; (ii) improved glucose tolerance; and (iii) disrupted lipid metabolism. In this chapter, we analyze the data currently available with respect to these three categories (Fig 4).

Proteins whose depletion causes deficient insulin signaling and glucose intolerance

There is extensive evidence of a major metabolic role of MFN2 in mouse tissues. Thus, muscle-specific ablation of *Mfn2* causes age-dependent glucose intolerance and deficient insulin signaling [166,167] (Fig 4A). *Mfn2*-deficient muscles also show reduced muscle autophagy, muscle atrophy, and loss of muscular function [167]. *Mfn2* repression in cultured muscle cells also reduces insulin signaling [142].

Mfn2 deficiency in liver is also associated with disrupted insulin signaling, enhanced hepatic glucose production, enhanced expression of gluconeogenic genes, and glucose intolerance [166]. *Mfn2* repression also reduces insulin signaling in human liver cells [27]. Notably, the phenotype linked to *Mfn2* deficiency is opposite to what occurs in mice upon ablation of *Mfn1*, which show protection against HFD-induced insulin resistance, and enhanced mitochondrial respiration [168]. These observations suggest that the mechanisms linked to *Mfn2* deficiency are not a consequence of alterations in mitochondrial fusion but are rather linked to its tethering function. *Mfn2* ablation in adipose tissues obtained by crossing *Mfn2*^{loxP/loxP} mice with mice expressing the Cre recombinase under the adiponectin promoter leads to enhanced body weight and fat mass, which was linked to a reduction in energy expenditure and in BAT thermogenesis [3]. In keeping with these data, BAT-specific *Mfn2* deletion through *Ucp1*-Cre causes BAT lipohypertrophy and cold intolerance [169]. The effects linked to *Mfn2* ablation in adipose depots are not detected upon ablation of *Mfn1* [3]. These findings thus support the notion that the alterations detected in BAT are not dependent on mitochondrial fusion, but on a different function of MFN1 and MFN2.

Specific ablation of *Mfn2* in pro-opiomelanocortin (POMC) neurons of the hypothalamus results in defective POMC processing, leptin resistance, hyperphagia, reduced energy expenditure, and obesity [156]. These data establish MFN2 in POMC neurons as an essential regulator of systemic energy balance. Along the same lines, interfering with mitochondrial fusion mechanisms in *Agrp* neurons by selectively knocking down *Mfn2* results in altered mitochondrial size and density in these cells. *Agrp*-specific *Mfn2* knockout mice gain less weight when fed a HFD due to decreased fat mass [170]. Available data in POMC neurons also indicate that the effects caused by *Mfn2* ablation differ greatly from what is detected for *Mfn1* ablation. Thus, mice lacking MFN1 in POMC neurons exhibit attenuated hypothalamic gene expression programs during the fast-to-fed transition [171]. This loss of mitochondrial flexibility in POMC neurons alters glucose sensing, causing abnormal glucose homeostasis as a result of defective insulin secretion by pancreatic β cells [171]. In conclusion, available data in conditional knockout mouse models indicate that *Mfn2* ablation causes defects in metabolism that are very different to those effects that result from ablation of *Mfn1*. These observations are compatible with MFN2 exerting metabolic effects in tissues via modulation of the mitochondria-ER contact sites.

In connection with the effects of the ER triggered by *Mfn2* deficiency, a potent UPR has been documented both in cells and in tissues [97,156,166]. Thus, *Mfn2* ablation in liver or in skeletal muscle causes chronic activation of the UPR, which involves the three UPR arms, i.e., the PERK, IRE-1a, and the ATF6 pathways [166]. Furthermore, treatment of liver-specific *Mfn2* knockout mice with an ER stress blocker restores insulin sensitivity and glucose homeostasis [166], thereby suggesting that the functional link between MFN2 and the UPR has metabolic relevance.

Ablation of *GRP75*, the bridge between IP3R and VDAC, has been reported to cause a reduction in VDAC1/IP3R1 interactions in human liver cells and in myotubes [27,142]. Moreover, *GRP75* deficiency reduces insulin signaling and insulin action in HuH7 liver cells [27,142] (Fig 4A). The depletion of *GRP75* in medullary thyroid carcinoma cells induces the MEK/ERK pathway and increases oxidative stress [172]. Both in *GRP75* knockdown SH-SY5Y bone marrow neuroblasts and in fibroblasts derived from a Parkinson's disease patient with *GRP75* loss of function, increased mitochondrial UPR (UPR^{MT}) was reported [173].

Hepatocyte-specific deletion of the tethering protein BAP31 is linked to metabolic defects in mice. *Bap31*-deficient mice show enhanced body weight, increased food intake, and greater liver steatosis after exposure to a HFD [174]. Another study with these mice reported the same effects upon tunicamycin treatment, as well as increased levels of ER-stress markers [175]. In *Bap31*-deficient mice, although not statistically significant, a trend toward increased p-eIF2 α , ATF4, and CHOP signaling was observed [175]. Moreover, hepatocytes of these mice show increased lipogenic gene expression and SREBP1C expression, and activation of SREBP signaling. *Bap31*-deficient mice show impaired glucose tolerance and reduced insulin responsiveness under normal diet or a HFD challenge (Fig 4A).

Depletion of the modulator of the permeability transition pore, *CypD*, in mice has been reported to enhance hepatic gluconeogenesis, as assessed by the pyruvate tolerance test [27]. In addition, *CypD* deficiency is associated with deficient insulin signaling and a reduced number of VDAC1/IP3R1 interactions in human liver cells [27]. The metabolic effects detected under conditions of *CypD* deficiency in mice and in human liver cells were characterized by UPR^{ER} [176]. In conclusion, these data are coherent with a model in which CYPD plays an important role in the maintenance of mitochondria-ER contact sites, which, upon dysregulation, trigger ER stress and metabolic alterations, namely deficient insulin signaling and insulin resistance (Fig 4A).

A shared feature of the absence of MFN2, *GRP75*, BAP31, or CYPD is the activation of UPR [97,156,166,173,175,176]. ER stress was initially proposed as a mechanism that drives insulin resistance-related diseases [177], and altered reticulum proteostasis alteration has also been in the spotlight as a possible driver of metabolic diseases [178]. Insulin resistance observed upon ablation of MFN2, *GRP75*, BAP31, or CYPD may arise as a result of altered mitochondria and/or ER protein homeostasis. The signaling pathways activated upon loss of protein homeostasis in both organelles converge in ATF4 and CHOP upregulation [179,180]. JNK activation is as well a consequence of ER stress that impairs insulin signaling, eventually leading to insulin resistance [177]. ER stress provokes hyperactivation of JNK, which phosphorylates and inhibits the insulin receptor IRS1 [177]. MFN2, BAP31, and CYPD ablation provoke an increase in activated JNK [156,175,176]; however, there

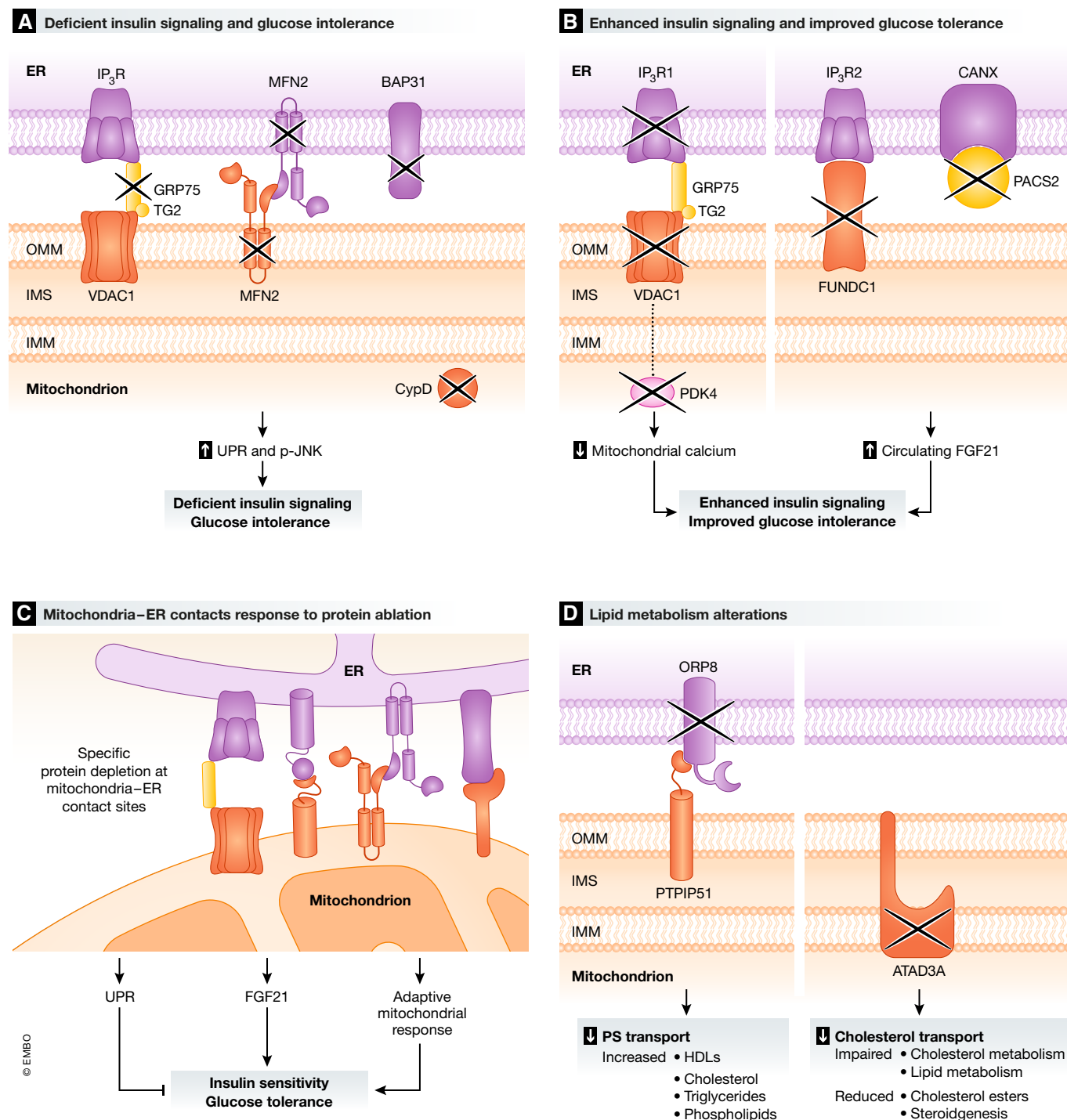


Figure 4. Metabolic impact of alterations in proteins participating in mitochondria-ER contacts.

(A) GRP75, MFN2, BAP31, or CypD depletion leads to deficient insulin signaling and glucose intolerance. The lack of GRP75, MFN2, BAP31, or CypD at mitochondria-ER contact sites causes deficient insulin signaling and glucose intolerance, probably through a mechanism that involves ^{ER}UPR or ^{mt}UPR . (B) IP3R1, VDAC1, FUNDC1, or PACS2 ablation results in enhanced insulin signaling and improved glucose tolerance. The mechanism by which FUNDC1 or PACS2 causes these effects is mediated by the release of FGF21. As a result of decreased mitochondrial Ca^{2+} accumulation, IP3R1 or VDAC1 ablation may result in enhanced insulin signaling and improved glucose tolerance. (C) Mitochondria-ER contacts response to protein ablation. The deletion of proteins that participate in the MAM results in the activation of signaling pathways that either enhance or impair insulin sensitivity and glucose tolerance. It has been proposed that these signaling pathways are related to UPR, FGF21, and an adaptive mitochondrial response that may lead to an improved or to a worsened response to insulin and glucose handling. (D) ORP8 or ATAD3A deficiency causes lipid metabolism alterations. Various alterations in lipid metabolism are observed upon ORP8 and ATAD3A ablation. ORP8 deficiency causes an increase in circulating HDL, cholesterol, triglycerides, and phospholipids. On the other hand, a lack of ATAD3A results in impaired cholesterol and lipid metabolism, reduced cholesterol esters, and decreased steroidogenesis.

are no data available on the levels of activated JNK in the absence of GRP75. Another common pathway that could be involved in insulin resistance upon depletion of *Mfn2*, *Grp75*, *Bap31*, or *CypD* is the MEK/ERK signaling cascade. MFN2 is a repressor of the MEK/ERK signaling pathway by its interaction with RAS [181]. ERK is hyperactivated upon *Mfn2* ablation in MEFs [182]. Ablation of *GRP75* stimulates the MEK/ERK signaling pathway in medullary thyroid carcinoma cells [172]. Moreover, the ERK signaling pathway is more active in *CypD* knockout mice hearts than in hearts of control animals [183]. Moreover, *BAP31* depletion in human embryonic stem cells leads to a mild increase in ERK phosphorylation [184]. Active ERK phosphorylates PPAR γ , which in turn stimulates the expression of genes related to diabetes [185,186].

Proteins whose depletion enhances insulin signaling and improves glucose tolerance

In addition to participating in mitophagy, FUNDC1 mediates the formation of mitochondria-ER contact sites and promotes Ca²⁺ flux from the ER to mitochondria through binding to IP3R2 in cardiac cells [76]. Cardiomyocyte-specific ablation of *Fundc1* results in decreased mitochondrial and cytosolic Ca²⁺ levels [76]. *Fundc1* ablation in mouse muscle causes mitochondrial dysfunction characterized by lower ATP and enhanced ROS [187]. In addition, *Fundc1*-ablated muscles show a reduced capacity to exercise, probably as a consequence of reduced fat oxidation [187]. Nevertheless, *Fundc1* knockout mice show improved glucose tolerance, insulin responsiveness, and less adiposity upon treatment with a HFD (Fig 4B). The process responsible for this reduced susceptibility to obesity is the activation of adaptive thermogenesis of adipose tissue driven by ROS-dependent muscle expression of FGF21 [187].

The downregulation of hepatic *Pacs2* in ob/ob mice increases maximal mitochondrial respiration and reduces JNK [29]. Under these conditions, *Pacs2* deficiency improves glucose tolerance and increases hepatic insulin signaling [29]. In oocytes from obese mice, genetic repression of *Pacs2* decreases Ca²⁺ influx into mitochondria and ROS production [158]. In *Pacs2* knockout mice, liver expression of FGF21 is increased and mice are resistant to diet-induced obesity [188] (Fig 4B).

FGF21 is a systemic regulator of energy homeostasis and insulin sensitivity [189]. Its expression is activated upon detection of low protein and high carbohydrate levels. In mouse models of diabetes, this protein improves insulin sensitivity and reduces circulating glucose and triglyceride levels [190]. FGF21 upregulation in *Fundc1*- and *Pacs2*-deficient mice explains the improvement in glucose handling and insulin signaling observed in these mice.

The inhibition of the anti-apoptotic protein BCL2 mimics glucose stimulation by increasing mitochondrial activity and ATP production in pancreatic b-cells [191]. Pancreatic islets isolated from *Bcl2*^{-/-} mice show enhanced insulin secretion in response to glucose stimulation [191]. The knockout of *Bak* and *Bax* in β -cells does not involve metabolic changes, indicating a role for BCL2 in metabolism besides its anti-apoptotic function [191]. In keeping with these results, induced insulin resistance in HepG2 cells upregulates BCL2 [192]. How *Bcl2* suppression leads to improved response to glucose has not been elucidated.

In contrast to the above data on the ablation of the Ca²⁺ channeling protein GRP75, adenoviral-induced hepatic deficiency of *Ip3r1* enhances mitochondrial respiration, lowers JNK activity, enhances

insulin signaling, and improves glucose tolerance in mice [29] (Fig 4B). Analysis of the *Ip3r1* heterozygous mutant (opt/C) mouse indicates defects in beta-pancreatic cells, with reduced beta-cell mass, and impaired glucose tolerance [193]. In oocytes from obese mice, genetic repression of *Ip3r1* reduces Ca²⁺ influx into mitochondria and also leads to a decrease in ROS production [158].

In line with these results, the downregulation of VDAC1 in pancreatic beta-cells has a protective effect against high glucose concentrations and maintains cellular reductive capacity [153]. *VDAC1* depletion in cancer cells has been shown to reprogram metabolism toward a decrease in energy production, accompanied by growth arrest [194,195]. Moreover, insulin release and ATP production in response to high glucose concentrations are improved in *VDAC1*-depleted cells [153]. In pancreatic islets from db/db mice, *VDAC1* inhibition leads to enhanced ATP generation and glucose-stimulated insulin secretion in response to high glucose levels [196] (Fig 4B).

To explain the hepatic increase in IP3R1-observed obese mice, in 2014 Arruda *et al* hypothesized that excessive Ca²⁺ accumulation in mitochondria was the cause of impaired glucose metabolism and insulin sensitivity. In the same study, they showed improved glucose tolerance when they knocked down IP3R1 [29]. Since the ablation of *VDAC1* in pancreatic cells also has a protective effect against high glucose concentrations [153], it is possible that decreased mitochondrial Ca²⁺ accumulation drives an improvement in insulin signaling.

Another important player in insulin signaling at the MAMs is mTORC2. mTORC2 signaling is essential for an adequate response to insulin [197]. Moreover, mTORC2 is implicated in the regulation of MAM integrity and its ablation results in decreased MAM formation and insulin resistance [90,197]. Insulin enhances mTORC2 localization at the MAMs [90]. Here, mTORC2 activation induces inhibitory phosphorylation of IP3R and PACS2 by AKT [90]. PACS2 ablation and IP3R ablation could have a synergistic effect with mTORC2 signaling in response to insulin stimuli.

Surprisingly, current data indicate that the repression of some proteins involved in mitochondria-ER contacts enhances glucose tolerance and insulin sensitivity by inducing the expression of FGF21, and perhaps by an independent mechanism related to an adaptive response of mitochondria which implies reduced mitochondrial Ca²⁺ or mTORC2 signaling. Further studies are required to determine whether those processes are indeed independent or whether they share common mechanisms.

Why the deletion of certain proteins that participate in mitochondria-ER contacts results in enhanced or in impaired insulin sensitivity and glucose tolerance is not known yet. We believe that the absence of these proteins stimulates several signaling pathways that are related to UPR, FGF21, and an adaptive mitochondrial response (Fig 4C). The final output, i.e., the observed phenotype, will depend in each case on the sum of all the pathways that have been activated. We propose that a sum of stimuli that results in UPR and therefore JNK activation will provoke impaired response to insulin and glucose handling. On the other hand, if the combination of all the stimuli leads to increased circulating FGF21 and/or an adaptive mitochondrial response (which would include decreased mitochondrial Ca²⁺ accumulation), the phenotype observed will be an improved response to insulin and glucose tolerance.

Proteins whose depletion alters lipid metabolism

Skeletal muscle-specific *Atad3* knockout mice show muscle atrophy in combination with mitochondrial abnormalities that include lack of cristae, reduced OXPHOS complexes and OPA1 expression, and progressive mtDNA depletion [198]. Fibroblasts derived from patients suffering from *ATAD3* gene cluster deletions show impaired cholesterol metabolism and mtDNA damage, as well as impaired lipid metabolism [199] (Fig 4D). In agreement with these data, muscle *ATAD3* deficiency reduces the levels of cholesterol esters in muscle, probably due to reduced Acetyl-CoA acetyltransferase [199]. The effects of *ATAD3* ablation on substrate handling have not been analyzed. Moreover, *ATAD3* ablation decreases steroidogenesis in a mouse cell line derived from Leydig cell tumor [200].

ORP5 and *ORP8* depletion leads to altered mitochondria morphology and function in HeLa cells [43]. The global ablation of *Orp8* in mice causes a marked elevation of high-density lipoprotein (HDL) cholesterol and phospholipids, which occurs in the absence of changes in apolipoprotein A-I [201]. Moreover, the secretion of nascent HDL particles is enhanced in primary *ORP8*-deficient hepatocytes, thereby suggesting altered biosynthesis of HDL [201] (Fig 4D). No information on the impact of *ORP8* depletion on glucose homeostasis is available.

In conclusion, available data suggest that some proteins of mitochondria-ER contacts play a pivotal role in the modulation of lipid metabolism. Future studies should address the mechanisms by which given proteins specifically modulate lipid metabolism in the absence of changes in energy metabolism.

Architectural, functional, and metabolic aspects of mitochondria-LD contact sites

Mitochondria and LDs are in active communication in highly metabolic tissues such as BAT, skeletal muscle, and heart [3,202–204]. It has been reported that the properties of the mitochondria surrounding LDs differ to those of mitochondria in the cytoplasm [2,205], which suggests a context-specific metabolic behavior of mitochondria. A study conducted by Benador *et al* [2] in BAT revealed that mitochondria surrounding LDs oxidize pyruvate, generate ATP, and use fatty acids for triacylglycerol (TAG) synthesis, whereas cytosolic mitochondria oxidize fatty acids. In addition, it has been reported in cultured cells that, under nutrient deprivation conditions, mitochondria and LDs interact in order to favor fatty acid oxidation [206,207]. This observation is in keeping with prior findings

indicating that lack of nutrients enhances fatty acid oxidation [208]. The variable impact of the interaction of LD with mitochondria on beta-oxidation will require a precise molecular explanation.

Proteins involved in mitochondria-LD contacts

The protein components of mitochondria-LD contact sites have been only partially characterized (Table 2). A tethering complex identified to operate in BAT is MFN2-PLIN1 [3] (MFN2 is located in the mitochondria and PLIN1 in LDs; Fig 5). Another mitochondrial protein that interacts with LD proteins is ACSL1 (acyl-CoA synthase long chain family member 1). BioID technology has revealed the interaction between ACSL1 and SNAP23 and VAMP4 in LDs [209] (Fig 5). The LD protein SNAP23 was first suggested to mediate the interaction between mitochondria and LDs since it was observed that its ablation reduced the contacts between these two organelles [210]. Moreover, SNAP23, together with VAMP4, is involved in LD fusion [211]. The LD protein PLIN5 has been described to localize at mitochondria-LD contacts; however, the mitochondrial partner of this protein is unknown [212,213]. PLIN5 interacts with ATGL and ABDH5 [214] on the LD surface (Fig 5).

Functional implications of the interaction between mitochondria and LDs

The associations between mitochondria and LDs influence LD size and mitochondrial dynamics. Thus, the interaction of mitochondria with LDs promotes the expansion of the latter [2]. PLIN5 overexpression increases mitochondrial recruitment to LDs and LD total area relative to control cells [2]. Mitochondrial morphology is also somehow regulated by interaction with LDs [2]: Mitochondria associated with LDs are more elongated than free mitochondria and contain reduced levels of DRP1 and cleaved OPA1 [2]. In turn, mitochondrial dynamics also influence LD size and distribution. Thus, impaired mitochondrial fusion causes an heterogeneous distribution of lipids throughout the mitochondrial network, greater accumulation of fatty acids in LDs, and increased fatty acid release from the cell [206]. This increase in fatty acids accumulation and release probably occurs due to impaired fatty acid oxidation in fragmented mitochondria.

PLIN5 is likely to promote the mitochondrial uptake of fatty acids since it interacts with adipose triglyceride lipase (ATGL) and its activator ABHD5 on the LD surface [214], leading to enhanced lipolysis. During glucose deprivation, ACSL1 interacts with SNAP23 and VAMP4 and thus increases mitochondria-LD contact sites [209]. Under these conditions, ACSL1 promotes the synthesis of acyl-CoA

Table 2. Mitochondria-LD contact sites proteins.

Protein	Location	Function in the mitochondria-LD contacts
ABDH5	LD	Lipolysis [214] (coupled to fatty acid transport into mitochondria?)
ACSL1	OMM	Mitochondria-LD tether (?)
ATGL	LD	Lipolysis [214] (coupled to fatty acid transport into mitochondria?)
MFN2	OMM	Mitochondria-LD tether [3] (?), Fatty acid transport into mitochondria [3] (?)
PLIN1	LD	Mitochondria-LD tether [3] (?), Fatty acid transport into mitochondria [3] (?)
PLIN5	LD, OMM	Fatty acid transport into mitochondria [214] (?)
SNAP23	LD	Mitochondria-LD tether [210] (?), LD fusion [211]
VAMP4	LD	Mitochondria-LD tether (?), LD fusion [211]

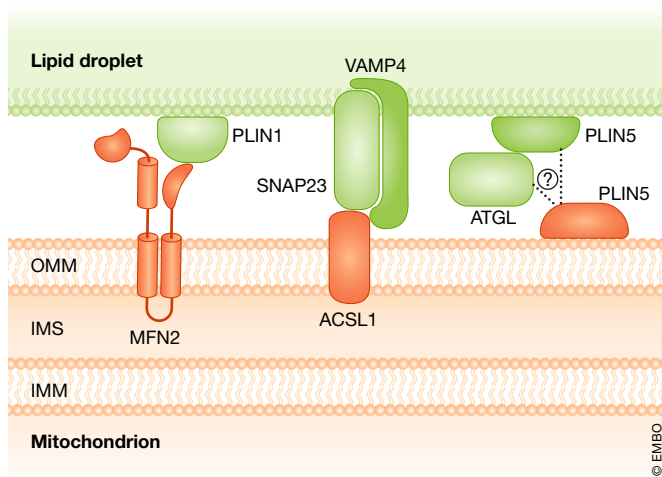


Figure 5. The architecture of mitochondria-LD contact sites.

Mitochondria establish contacts with lipid droplets (LDs). Although these contacts are poorly studied, several proteins have been found to participate in them. MFN2 in mitochondria interacts with the LD protein PLIN1. Mitochondrial ACSL1 has been found to form a complex with SNAP23 and VAMP4, both present on the LD surface. Moreover, PLIN5 has been found both on the surface of LDs and in the OMM. It is known that PLIN5 interacts with ATGL; however, the protein complex through which PLIN5 anchors LDs to mitochondria is still uncharacterized.

from fatty acids released by LDs, which are then channeled through mitochondrial beta-oxidation. Such a process may sustain the thermogenic capacity of BAT during its activation [215].

The MFN2-PLIN1 complex may be key for the maintenance of fatty acid oxidation in BAT and thus for thermogenesis [3]. Moreover, proteomic analysis of the LD-enriched fraction of BAT has identified the mitochondrial thermogenic protein UCP1 upon cold treatment [205], thereby suggesting increased cooperation of mitochondria and LDs for heat production.

Mitochondria-LD contacts respond to metabolic alterations

Mitochondria-LD contacts are modulated by nutrient availability in various tissues. Thus, glucose deficiency promotes LD interaction with mitochondria in monkey kidney Vero cells and in mouse primary hepatocytes [209,216]. The interaction of ACSL1 with SNAP23 and VAMP4 is enhanced upon glucose deprivation in mouse primary hepatocytes [209]. In agreement with these observations, SNAP23 expression increases in rat livers during fasting [217]. Proteomic analysis of purified LDs from mouse livers revealed that PLIN5 and ACSL1 proteins are more abundant in fasted mice [218]. It is likely that the enhanced mitochondria-LD contacts favor fatty acid oxidation in mitochondria under conditions of nutrient deprivation or during physiological fasting.

Mitochondria-LD contacts are also modified in BAT under conditions of thermogenic activity. In this regard, Benador *et al* [2] reported a 50% decrease in mitochondria contacts with LDs in primary cultures of BAT from mice maintained at 6°C compared to BAT of mice under thermoneutral conditions. In contrast, Boutant *et al* [3] observed that PLIN1-MFN2 interaction is enhanced upon treatment with an adrenergic agonist in brown adipocytes. In

agreement with the latter findings, Yu *et al* [205] detected increased expression of PLIN1 and ATGL in BAT of mice subjected to cold. No explanation for the reduced mitochondria-LD interaction upon cold exposure, under conditions which are linked to greater beta-oxidation, has been put forward to date.

The effects of a HFD, obesity, diabetes, and exercise on mitochondria-LD apposition have not been studied in depth. However, it has been reported that these conditions have an impact on proteins that operate at the interface of these two organelles. PLIN1 protein levels are decreased in the WAT of mice on a HFD in comparison with that of animals on a normal chow diet [219]. In skeletal muscle, two independent studies found that PLIN5 protein expression is increased in mice upon exposure to a HFD [220,221]. These findings are in agreement with a study performed in human muscle biopsies, in which PLIN5 protein levels were higher in obese and diabetic patients compared to those of healthy subjects [222].

Exercise influences the expression of proteins located at the mitochondria-LD interface. Both control and HFD-fed mice subjected to chronic exercise show increased levels of muscle PLIN1 [221]. Furthermore, the levels of this protein are higher in trained HFD-fed mice compared to trained mice under a normal diet. Interestingly, triglycerides tended to accumulate more in the muscle of trained animals and of those on HFD.

In turn, PLIN5 is upregulated in the primary myotubes of physically active subjects upon lipolytic stimulation [223]. In agreement with this, PLIN5-positive LDs are higher in muscle sections from trained individuals and total PLIN5 is higher in these subjects [222]. Upregulation of PLIN1 and PLIN5 in skeletal muscle of trained subjects may participate in the increased contacts that occur between mitochondria and LDs.

Metabolic impact of alterations in proteins participating in mitochondria-LD contacts

Disruption of the contacts between mitochondria and LDs may affect metabolism. However, information in this regard is scarce. Some animal and cellular models lacking proteins involved in these contacts have been generated, but the effects observed may not be fully attributable to the disruption of mitochondria-LD contact sites.

The specific ablation of *Mfn2* in BAT in mice impairs lipolysis, fatty acid oxidation, and respiration, and thus decreases the thermogenic capacity of this tissue [3]. Moreover, that study showed that the lack of MFN2 disrupts fatty acid flux into mitochondria, probably as a result of impairment of mitochondria and LD contacts. *Mfn2*-deficient BAT shows an enhanced expression of FGF21 when mice are subjected to a HFD, leading to increased circulating levels of FGF21. Whether FGF21 induction is due to cellular stress that is specifically dependent on alterations in mitochondria-LD contacts or to other biological effects of MFN2 remains unknown. However, under these conditions, the enhanced levels of FGF21 protect *Mfn2* knockout mice against lipid accumulation in the liver and lead to improved hepatic fatty acid oxidation.

Liver-specific *Plin5* knockout mice show reduced mitochondria-LDs contacts in hepatocytes, decreased fatty acid oxidation, and reduced triglyceride secretion [224]. Treatment of these mice with a HFD induces greater accumulation of TAG, the activation of JNK, and insulin resistance. Partial ablation of *Plin5* in muscle leads to insulin resistance with improved insulin responsiveness under HFD feeding [220]. Complete ablation of *Plin5* in skeletal

muscle results in glucose intolerance, insulin resistance in adipose tissue, and reduced circulating insulin levels [225]. After HFD feeding, *Plin5* knockout animals show decreased ER stress markers (p-IRE1 α , spliced XBP1, *Atf4*), reduced activation of JNK, and diminished levels of proinflammatory markers (*Tnfa*, *Il6*, *Ccl2*), as well as decreased levels of muscle, circulating, and hepatic FGF21 compared to wild-type mice. These metabolic alterations are reversed upon injection of recombinant FGF21. Moreover, in agreement with these findings, *Plin5* overexpression in skeletal muscle causes increased energy metabolism and accumulation of more TAG in skeletal muscle under conditions of normal glucose and insulin tolerance [226]. Upon HFD, the expression of inflammatory markers in the liver is lower and muscle and plasma levels of FGF21 are increased. Moreover, when mice overexpressing *Plin5* are subjected to a HFD, they show upregulation of browning markers (*Ucp1*, *Cidea*, *Adiponectin*, *Cebpa*) in WAT, in comparison with wild-type mice. In line with these results, another study found that overexpression of *PLIN5* reduces lipolysis and fatty acid oxidation and increases glycogen synthesis and glucose oxidation in human primary myotubes [220]. Nevertheless, augmented energy demand by forskolin application increases lipid oxidation in conditions of *PLIN5* overexpression to a higher rate than in control myotubes. Laurens *et al* proposed that higher energy demands increase the contacts between mitochondria and LDs in order to optimize fatty acid oxidation and that HFD uncouples LD from mitochondria.

Total *Plin1* knockout mice are resistant to insulin [219]. Livers of *Plin1* knockout mice show spontaneous hepatosteatosis, impaired glucose metabolism, increased synthesis of TAG, and decreased fatty acid oxidation [227]. Furthermore, these mice suffer from hypertrophic cardiomyopathy [228] and increased atherosclerosis [229]. The depletion of *Plin1* causes increased circulating levels of proinflammatory cytokines, TAGs, and free fatty acids accompanied by white adipose tissue inflammation with higher M1 macrophage infiltration [219]. This proinflammatory phenotype is driven by enhanced lipolysis in adipocytes, which leads to increased production and the release of prostaglandins.

Snap23 knockdown in HL-1 cardiomyocytes causes insulin resistance *in vitro* [211]. In the same study, wild-type HL-1 cells exposed to oleic acid showed increased recruitment of SNAP23 to LDs and insulin resistance. Insulin resistance was rescued by *Snapp23* overexpression. Since SNAP23 also localizes to the plasma membrane where it translocates GLUT4, insulin resistance might be caused by the absence of this protein in the plasma membrane.

Functional and metabolic aspects of mitochondria–lysosome contact sites

The interaction between mitochondria and lysosomes has been widely studied upon stress or mitochondrial damage conditions. Damaged mitochondria are degraded by selective autophagy (mitophagy), and this process implies the fusion of the mitophagosome with a lysosome (reviewed by Nguyen *et al* [230]). Moreover, mitochondria generate vesicles that trigger lysosomes, mitochondria-derived vesicles (MDVs), and this process is considered as a way for mitochondria to degrade proteins or oxidized components (reviewed by Sugiura *et al* [231]). Besides these studies performed

under stress conditions and revealing indirect interaction between mitochondria and lysosomes, little is known about physical apposition of mitochondria and lysosomes in basal conditions. In this section, we review the recent advances on this field and we analyze the functional aspects of the apposition between lysosomes and mitochondria and its crosstalk with metabolism.

Composition and functions of contacts between mitochondria and lysosomes

Over the past decade, although physical interaction between mitochondria and lysosomes had not yet been described, there was evidence for mitochondria and lysosome crosstalk since disruption of mitochondria affects lysosomal function and dynamics and lysosomal damage triggers mitochondrial homeostasis impairment (reviewed by Raimundo *et al* [232]). Recently, cutting-edge microscopy studies have detected the establishment of physical contacts between lysosomes and mitochondria in healthy cells in the absence of damage stimulus [1,233]. Besides, the latest discoveries in the field point to RAB7 as a master coordinator of these contacts [6,7,234–236] (Fig 6).

Lysosome–mitochondria contacts are promoted by GTP-bound lysosomal RAB7 [6]. When a constitutively active GTP-bound RAB7 mutant is expressed, contacts between lysosomes and mitochondria increase and these are more stable over time. TBC1D15 is a GTPase activating protein that governs RAB7 activity [237]. Recruitment of TBC1D15 to mitochondria by FIS1 favors GTP hydrolysis and separates lysosomes from mitochondria [6] (Fig 6). TBC1D15 inactive mutants can still be recruited to mitochondria; however, they do not uncouple mitochondria from lysosomes and lysosomes become larger [6]. Interaction between RAB7 and TBC1D15 has not been described yet. Confocal microscopy has revealed colocalization between lysosomes and sites for mitochondrial division [6] in which, as we described before, ER tubules participate [58]. These findings suggest that the interface between these two organelles plays a major role in the regulation of mitochondrial and lysosomal dynamics.

It has been discovered in retinal ganglion cells of *Xenopus laevis* embryos that late endosomes can associate with ribosomes in axons through RAB7 and RAB5 and protein translation can occur at the endosomal membrane [235]. Some mitochondrial proteins such as VDAC2 can be translated at the surface of these late endosomes and then be transferred to mitochondria [235] (Fig 6). Mutations in *rab7* associated with Charcot–Marie–Tooth disease cause downregulation of mitochondrial protein translation, mitochondrial elongation, and diminished mitochondrial membrane potential in the axons [235]. Currently, the proteins in the interorganellar surface that contribute to mitochondrial incorporation of the newly synthesized peptides remain unknown.

Melanogenesis is a process influenced by the apposition between melanosomes and mitochondria [7]. Melanosomes, which are lysosomal related organelles that accumulate melanin in pigmented cells, establish contacts with mitochondria through MFN2 in melanocytes [7] (Fig 6). However, the melanosomal component of these junctions remains unknown. MFN2 ablation decreases the interaction between mitochondria and melanosomes and arrests melanogenesis activation [7].

The interface between mitochondria and lysosomes could play a role in autophagy. It is known that MFN2 interacts with RAB7 in mouse hearts [234] (Fig 6). This interaction increases upon

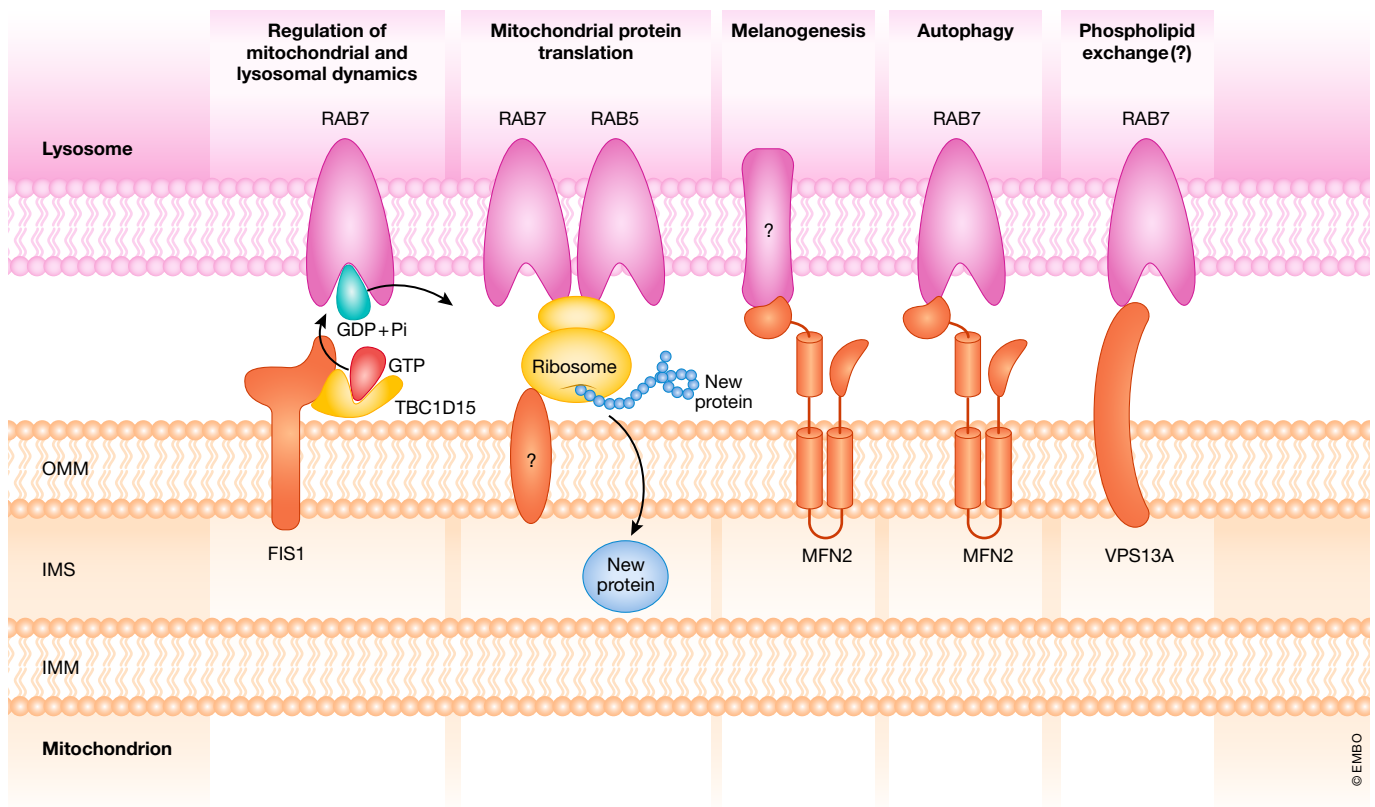


Figure 6. Mitochondria–lysosome interface.

Several processes take place at the contacts between mitochondria and lysosomes: (A) Regulation of mitochondrial and lysosomal dynamics by RAB7, TBC1D15, and FIS1 coordination; (B) mitochondrial protein translation in ribosomes anchored to the endosomal surface by interaction with RAB7 and RAB5 in close proximity to mitochondria; (C) melanogenesis in melanosomes that interact with mitochondria through MFN2; (D) autophagosome to lysosome fusion, which is supported by MFN2–RAB7 interaction; and (E) possible phospholipid exchange through VPS13A interaction with RAB7.

autophagy induction by starvation and has been proposed to be key for autophagosome–lysosome fusion [234].

A recent study indicates that lysosomal RAB7 immunoprecipitates and partially colocalizes with mitochondrial VPS13A in HeLa cells and that the absence of VPS13A causes impaired lysosomal degradation [236]. Moreover, a different study has identified a hydrophobic cavity in the structure of this protein and has proved its capacity to bind and transfer phospholipids between two membranes [238]. However, it has not been elucidated whether mitochondria and lysosomes exchange phospholipids in a non-vesicular manner (Fig 6).

A long DRP1 isoform present in mitochondria, lysosomes, and plasma membrane is highly enriched in mitochondrial contacts with lysosomes [239]. This isoform is mainly expressed in the brain and conserves mitochondrial division capacity [239]. When overexpressed in MEF, DRP1 long isoform colocalizes with RAB7; nevertheless, it is not known whether RAB7 and DRP1 interact [239]. GTPase activity and oligomerization capacity of DRP1 long isoform are necessary for its localization to lysosomes [239]. The role of this isoform of DRP1 in membrane junctions remains uncharacterized, although a role in lysosomal dynamics has already been discarded [239].

Besides the participation of mitochondria–lysosome contacts in organelle dynamics regulation, mitochondrial protein translation

and melanogenesis, and their possible contribution to autophagy and phospholipid exchange, communication between mitochondria and lysosomes has been associated with iron translocation to mitochondria [240] and lipofuscin deposit formation in lysosomes [241]. Nevertheless, mechanisms for these processes are poorly described and it is not known whether they take place in a vesicular or non-vesicular manner.

The effects of mitochondria–lysosome contact modification on metabolism

Little is known about how the modification of the contacts between mitochondria and lysosomes affects metabolism. RAB7 role in fat storage has been reported in *C. elegans*, in which neuronal silencing of *rab7* results in reduced fat storage [242]. *Rab7* knockdown in mouse bone marrow cells decreases glucose consumption and ROS excess [243]. The knockout of *TBC1D15* decreases glucose uptake in L02 human fetal hepatocytes [244]. Moreover, *TBC1D15* ablation reduces GLUT4 mRNA and protein levels and this effect is more dramatic in the presence of insulin [244]. In the absence of *TBC1D15*, GLUT4 colocalizes with lysosomes, where it could be degraded [244]. The authors suggest that *TBC1D15* is necessary for GLUT4 translocation to the plasma membrane. There are no studies

Box: In need of answers

- (i) What is the precise composition of tethering (and spacer) complexes responsible for the contacts of mitochondria with other organelles (ER, lipid droplets, lysosomes, Golgi, peroxisomes, etc.)?
- (ii) How do the tethering (and spacer) complexes undergo modulation in a tissue-specific manner in response to hormonal or nutritional alterations? What are the mechanisms involved?
- (iii) Do the tethering complexes functionally interact with other tethering/spacer complexes or with functional proteins present in contacts? If so, what is the nature of the mechanisms involved?
- (iv) Identification of the precise functions operating in the different contact sites, and characterization of the complexes involved in the catalysis present in those contacts. Analysis of the modes of regulation of the functional complexes in response to hormonal and/or nutritional cues.
- (v) What are the mechanisms by which mitochondria within a specific cell type show a heterogeneous interaction with specific organelles such as lipid droplets?
- (vi) Because some of the proteins involved in tethering or in function in contact sites are present in multiple locations in cells, there is a need to design strategies to identify the specific function of the protein located in the contact site rather in other locations.
- (vii) How do alterations in proteins present in contact sites impact on metabolic homeostasis? Why do some proteins mediate enhanced anabolism whereas others mediate inhibited anabolism, and other alterations in lipid metabolism? What is the physiological meaning, and what the mechanisms in place?

linking these observations on RAB7 and TBC1D15 with mitochondria–lysosome interaction.

Impact of metabolism on mitochondria–lysosome contacts

The influence of metabolic homeostasis on mitochondria–lysosome contacts in mammalian cells is an unexplored field. Related findings have been discovered in yeast [245]. Yeast vacuoles interact with mitochondria through Ypt7, the yeast homologue of RAB7, and Vps39 in the vacuole [245] and Tom40 in the mitochondria [246]. In the absence of glucose, vacuole–mitochondria contacts are lost, but upon addition of glucose to the growth medium, these contacts slowly reappear [245]. This study is the first evidence that glucose levels modulate mitochondria–lysosome contacts in yeast cells; nevertheless, more insight is necessary into how glucose deprivation affects these contacts in mammalian cells.

Under insulin or amino acid stimuli in mammalian cells, lysosomal mTORC1 is activated and stimulates mitochondrial oxidative pathways and mtDNA synthesis [247]. RAB7 interacts with mTOR in mouse bone marrow cells [243]. It is not known whether this interaction occurs in other cell types. Given the importance of mTOR in response to nutrient availability and RAB7 in the interaction between mitochondria and lysosomes, this complex is a potential candidate to modulate mitochondria–lysosome contacts in response to metabolism.

Contacts of mitochondria with peroxisomes and the Golgi apparatus

Peroxisomes and mitochondria establish physical contacts, and this interaction influences cell metabolism [1,8,248]. ECI2, a

peroxisomal enoyl-CoA isomerase, is so far the only protein established as part of a mitochondria–peroxisome tethering complex [8]. A proximity ligation assay has revealed that peroxisomal ECI2 and mitochondrial TOM20 interact in MA-10 Leydig-like cells [8], although more precise analyses of this interaction such as co-immunoprecipitation or two-hybrid screening have not been performed. Overexpression of *ECI2* results in increased steroid biosynthesis [8], a metabolic process that takes place in mitochondria. Moreover, MAMs associate with peroxisomes during antiviral immune signaling [249,250]. Beta-oxidation needs the interplay between both compartments: Very long chain fatty acids (> 16 carbons) are shortened in peroxisomes (to 6–8 carbons fatty acids) and then preferentially translocated to mitochondria for complete oxidation [251]. How shortened fatty acids are shuttled from peroxisomes to mitochondria remains unknown.

Golgi apparatus and mitochondria also communicate with each other by physical interaction [1,4]. Nevertheless, the key players of this apposition remain unknown. The existence of Ca^{2+} gradients from the Golgi apparatus to mitochondria has been discovered in pancreatic acinar cells [4], although the existence of calcium channels for active or passive calcium transport has not been clarified yet.

Future perspectives

The interaction between organelles is an emerging field that is gaining importance due to the physiological implications of organelle contact sites. In this regard, mitochondria contacts with the ER are the better characterized ones to date and their functional and metabolic aspects have already been highlighted. Nevertheless, the full composition of tethering complexes still needs to be discovered. Mitochondria interacting with lipid droplets show different metabolic behavior compared with those mitochondria that are free in the cytosol. Studies on the interaction of LD and mitochondria have generated two hypotheses: The first hypothesis is that mitochondria–LD interaction favors beta-oxidation, and the second hypothesis is that mitochondria–LD interaction results in increased TAG synthesis. More insight is needed to determine whether metabolic behavior of mitochondria associated with LDs depends on the energetic demands of the tissue or the whole body. Lysosome–mitochondria contacts in mammalian cells are still poorly described but currently in the spotlight of research. Whether reciprocal dynamics regulation exerted between mitochondria and lysosomes has any metabolic implications is yet to be discovered. The key players in the communication between mitochondria and peroxisomes have not been deciphered. Future characterization of this interaction will be metabolically relevant since peroxisomes and mitochondria interact during beta-oxidation of fatty acids. Although several studies have revealed an interaction between mitochondria and the Golgi apparatus, the functional and structural features of this interaction remain unknown. How Ca^{2+} is transferred from the Golgi apparatus to mitochondria and what Ca^{2+} flux between these organelles signals for has not been discovered yet. It is possible that metabolic features of mitochondria could depend on their interaction with other organelles, which we hypothesize would be determined by the organ or tissue energetic requirements. A tissue-/cell-specific characterization of

contact sites is lacking, but it will be fundamental for a better understanding of contact sites influence on metabolism. Future discoveries on organelle contact sites will fill these gaps and transform our understanding of cellular physiology and metabolism regulation and likely will provide us with new tools for targeting metabolic disorders.

Acknowledgements

I.G. is a recipient of a PhD fellowship from the Ministerio de Economía y Competitividad (MINECO). This study was supported by research grants from the MINECO (SAF2016-75246R), the Generalitat de Catalunya (Grant 2017SGR1015), INFLAMES (PIE-14/00045, Instituto de Salud Carlos III, CIBERDEM ("Instituto de Salud Carlos III"), the Marató de TV3, the Fundación BBVA, and the Fundación Ramon Areces. We gratefully acknowledge institutional funding from MINECO through the Centres of Excellence Severo Ochoa Award, and from the CERCA Programme of the Generalitat de Catalunya.

Conflict of interest

The authors declare that they have no conflict of interest.

References

- Valm AM, Cohen S, Legant WR, Melunis J, Hershberg U, Wait E, Cohen AR, Davidson MW, Betzig E, Lippincott-Schwartz J (2017) Applying systems-level spectral imaging and analysis to reveal the organelle interactome. *Nature* 546: 162–167
- Benador IY, Veliova M, Mahdavian K, Petcherski A, Wikstrom JD, Assali EA, Acín-Pérez R, Shum M, Oliveira MF, Cinti S et al (2018) Mitochondria bound to lipid droplets have unique bioenergetics, composition, and dynamics that support lipid droplet expansion. *Cell Metab* 27: 869–885.e6
- Boutant M, Kulkarni SS, Joffraud M, Ratajczak J, Valera-Alberni M, Combe R, Zorzano A, Cantó C (2017) Mfn2 is critical for brown adipose tissue thermogenic function. *EMBO J* 36: 1543–1558
- Dolman NJ, Gerasimenko JV, Gerasimenko OV, Voronina SG, Petersen OH, Tepikin AV (2005) Stable Golgi-mitochondria complexes and formation of Golgi Ca^{2+} gradients in pancreatic acinar cells. *J Biol Chem* 280: 15794–15799
- Marsh BJ, Mastronarde DN, Buttle KF, Howell KE, McIntosh JR (2001) Organellar relationships in the Golgi region of the pancreatic beta cell line, HIT-T15, visualized by high resolution electron tomography. *Proc Natl Acad Sci USA* 98: 2399–2406
- Wong YC, Ysselstein D, Krainc D (2018) Mitochondria-lysosome contacts regulate mitochondrial fission via RAB7 GTP hydrolysis. *Nature* 554: 382–386
- Daniele T, Hurbain I, Vago R, Casari G, Raposo G, Tacchetti C, Schiaffino MV (2014) Mitochondria and melanosomes establish physical contacts modulated by Mfn2 and involved in organelle biogenesis. *Curr Biol* 24: 393–403
- Fan J, Li X, Issop L, Culty M, Papadopoulos V (2016) ACBD2/ECI2-mediated peroxisome-mitochondria interactions in Leydig cell steroid biosynthesis. *Mol Endocrinol* 30: 763–782
- De Vos KJ, Mórocz GM, Stoica R, Tudor EL, Lau KF, Ackerley S, Warley A, Shaw CE, Miller CCJ (2012) VAPB interacts with the mitochondrial protein PTP1B1 to regulate calcium homeostasis. *Hum Mol Genet* 21: 1299–1311
- Szabadkai G, Bianchi K, Várnai P, De Stefani D, Wieckowski MR, Cavagna D, Nagy AI, Balla T, Rizzuto R (2006) Chaperone-mediated coupling of endoplasmic reticulum and mitochondrial Ca^{2+} channels. *J Cell Biol* 175: 901–911
- Iwasawa R, Mahul-Mellier AL, Datler C, Pazarentzos E, Grimm S (2011) Fis1 and Bap31 bridge the mitochondria-ER interface to establish a platform for apoptosis induction. *EMBO J* 30: 556–568
- de Brito OM, Scorrano L (2008) Mitofusin 2 tethers endoplasmic reticulum to mitochondria. *Nature* 456: 605–610
- Stoica R, De Vos KJ, Paillusson S, Mueller S, Sancho RM, Lau KF, Vizcay-Barrena G, Lin WL, Xu YF, Lewis J et al (2014) ER-mitochondria associations are regulated by the VAPB-PTPIP51 interaction and are disrupted by ALS/FTD-associated TDP-43. *Nat Commun* 5: 3996
- Di Mattia T, Wilhelm LP, Ikhlef S, Wendling C, Spehner D, Nominé Y, Giordano F, Mathelin C, Drin G, Tomasetto C et al (2018) Identification of MOSPD2, a novel scaffold for endoplasmic reticulum membrane contact sites. *EMBO Rep* 19: e45453
- Thoudam T, Ha C, Leem J, Chanda D, Park J, Kim H, Jeon J-H, Choi Y-K, Liangpunsakul S, Huh YH et al (2019) PDK4 augments ER – mitochondria contact to dampen skeletal muscle insulin signaling during obesity. *Diabetes* 68: 571–586
- Yoon Y, Krueger EW, Oswald BJ, McNiven MA (2003) The mitochondrial protein hFis1 regulates mitochondrial fission in mammalian cells through an interaction with the dynamin-like protein DLP1. *Mol Cell Biol* 23: 5409–5420
- Breckenridge DG, Stojanovic M, Marcellus RC, Shore GC (2003) Caspase cleavage product of BAP31 induces mitochondrial fission through endoplasmic reticulum calcium signals, enhancing cytochrome c release to the cytosol. *J Cell Biol* 160: 1115–1127
- Chen H, Detmer SA, Ewald AJ, Griffin EE, Fraser SE, Chan DC (2003) Mitofusins Mfn1 and Mfn2 coordinately regulate mitochondrial fusion and are essential for embryonic development. *J Cell Biol* 160: 189–200
- Santel A, Fuller MT (2001) Control of mitochondrial morphology by a human mitofusin. *J Cell Sci* 114: 867–874
- Hamasaki M, Furuta N, Matsuda A, Nezu A, Yamamoto A, Fujita N, Oomori H, Noda T, Haraguchi T, Hiraoka Y et al (2013) Autophagosomes form at ER-mitochondria contact sites. *Nature* 495: 389–393
- Filadi R, Greotti E, Turacchio G, Luini A, Pozzan T, Pizzo P (2015) Mitofusin 2 ablation increases endoplasmic reticulum – mitochondria coupling. *Proc Natl Acad Sci USA* 112: E2174–E2181
- Santos Leal N, Schreiner B, Moreira C, Filadi R, Wiehager B, Karlstr H, Pizzo P, Ankarcrona M (2016) Mitofusin-2 knockdown increases ER – mitochondria contact and decreases amyloid β -peptide production. *J Cell Mol Med* 20: 1686–1695
- Naon D, Zaninello M, Giacomello M, Varanita T, Grespi F, Lakshminarayanan S, Serafini A, Semenzato M, Herkenne S, Hernández-Alvarez MI et al (2016) Critical reappraisal confirms that Mitofusin 2 is an endoplasmic reticulum-mitochondria tether. *Proc Natl Acad Sci USA* 113: 11249–11254
- McClelland G, Goiran T, Yi W, Chen CX, Lauinger ND, Krahn AI, Valimehr S, Rakovic A, Rouiller I, Durcan TM (2018) Mfn2 ubiquitination by PINK1/parkin gates the p97-dependent release of ER from mitochondria to drive mitophagy. *Elife* 7: 1–35
- Teng Y, Ren X, Li H, Shull A, Kim J, Cowell JK (2016) Mitochondrial ATAD3A combines with GRP78 to regulate the WASF3 metastasis-promoting protein. *Oncogene* 35: 333–343
- Honrath B, Metz I, Bendridi N, Rieusset J, Culmsee C, Dolga AM (2017) Glucose-regulated protein 75 determines ER-mitochondrial coupling

- and sensitivity to oxidative stress in neuronal cells. *Cell Death Discov* 3: 17076
27. Tubbs E, Theurey P, Vial G, Bendridi N, Bravard A, Chauvin MA, Ji-Cao J, Zoulim F, Bartosch B, Ovize M et al (2014) Mitochondria-associated endoplasmic reticulum membrane (MAM) integrity is required for insulin signaling and is implicated in hepatic insulin resistance. *Diabetes* 63: 3279–3294
 28. Paillard M, Tubbs E, Thiebaut PA, Gomez L, Fauconnier J, Da Silva CC, Teixeira G, Mewton N, Belaidi E, Durand A et al (2013) Depressing mitochondria-reticulum interactions protects cardiomyocytes from lethal hypoxia-reoxygenation injury. *Circulation* 128: 1555–1565
 29. Arruda AP, Pers BM, Parlakgöl G, Güney E, Inouye K, Hotamisligil GS (2014) Chronic enrichment of hepatic endoplasmic reticulum-mitochondria contact leads to mitochondrial dysfunction in obesity. *Nat Med* 20: 1427–1435
 30. Eletto MD, Rossin F, Occhigrossi L, Pinton P, Eletto MD, Rossin F, Occhigrossi L, Farrace MG, Faccenda D, Desai R (2018) Transglutaminase type 2 regulates ER-mitochondria contact sites by interacting with report transglutaminase type 2 regulates ER-mitochondria contact sites by interacting with GRP75. *Cell Rep* 25: 3573–3581
 31. Qiao X, Jia S, Ye J, Fang X, Zhang C, Cao Y, Xu C, Zhao L, Zhu Y, Wang L et al (2017) PTPIP51 regulates mouse cardiac ischemia/reperfusion through mediating the mitochondria-SR junction. *Sci Rep* 7: 1–14
 32. Chiang SF, Huang CY, Lin TY, Chiou SH, Chow KC (2012) An alternative import pathway of AIF to the mitochondria. *Int J Mol Med* 29: 365–372
 33. Ainbinder A, Boncompagni S, Protasi F, Dirksen RT (2015) Role of mitofusin-2 in mitochondrial localization and calcium uptake in skeletal muscle. *Cell Calcium* 57: 14–24
 34. Kentala H, Weber-Boyvat M, Olkkonen VM (2016) OSBP-related protein family: mediators of lipid transport and signaling at membrane contact sites. *Int Rev Cell Mol Biol* 321: 299–340
 35. Kuge O, Nishijima M (1997) Phosphatidylserine synthase I and II of mammalian cells. *Biochim Biophys Acta* 1348: 151–156
 36. McMurray W (1986) Origins of the phospholipids in animal mitochondria. *Biochem Cell Biol* 64: 1115–1124
 37. Vance JE (1991) Newly made phosphatidylserine and phosphatidylethanolamine are preferentially translocated between rat liver mitochondria and endoplasmic reticulum. *J Biol Chem* 266: 89–97
 38. Dennis EA, Kennedy EP (1972) Intracellular sites of lipid synthesis and the biogenesis of mitochondria. *J Lipid Res* 13: 263–267
 39. Blusztajn JK, Zeisel SH, Wurtman RJ (1979) Synthesis of lecithin (phosphatidylcholine) from phosphatidylethanolamine in bovine brain. *Brain Res* 179: 319–327
 40. Vance JE (1990) Phospholipid synthesis in a membrane fraction associated with mitochondria. *J Biol Chem* 265: 7248–7257
 41. Du X, Kumar J, Ferguson C, Schulz TA, Ong YS, Hong W, Prinz WA, Parton RG, Brown AJ, Yang H (2011) A role for oxysterol-binding protein-related protein 5 in endosomal cholesterol trafficking. *J Cell Biol* 192: 121–135
 42. Chung J, Torta F, Masai K, Lucast L, Czaplá H, Tanner LB, Narayanaswamy P, Wenk MR, Nakatsu F, De Camilli P (2015) PI4P/phosphatidylserine countertransport at ORP5- and ORP8-mediated ER–plasma membrane contacts. *Science* 349: 428–432
 43. Galmes R, Houcine A, van Vliet AR, Agostinis P, Jackson CL, Giordano F (2016) ORP5/ORP8 localize to endoplasmic reticulum-mitochondria contacts and are involved in mitochondrial function. *EMBO Rep* 17: 800–810
 44. AhYoung AP, Jiang J, Zhang J, Khoi Dang X, Loo JA, Zhou ZH, Egea PF (2015) Conserved SMP domains of the ERMES complex bind phospholipids and mediate tether assembly. *Proc Natl Acad Sci USA* 112: E3179–E3188
 45. Schauder CM, Wu X, Saheki Y, Narayanaswamy P, Torta F, Wenk MR, De Camilli P, Reinisch KM (2014) Structure of a lipid-bound extended synaptotagmin indicates a role in lipid transfer. *Nature* 510: 552–555
 46. Hirabayashi Y, Kwon SK, Paek H, Pernice WM, Paul MA, Lee J, Erfani P, Raczkowski A, Petrey DS, Pon LA et al (2017) ER-mitochondria tethering by PDZD8 regulates Ca²⁺ dynamics in mammalian neurons. *Science* 358: 623–630
 47. Elustondo P, Martin LA, Karten B (2017) Mitochondrial cholesterol import. *Biochim Biophys Acta* 1862: 90–101
 48. Prasad M, Kaur J, Pawlak KJ, Bose M, Whittall RM, Bose HS (2015) Mitochondria-associated endoplasmic reticulum membrane (MAM) regulates steroidogenic activity via steroidogenic acute regulatory protein (StAR)-voltage-dependent anion channel 2 (VDAC2) interaction. *J Biol Chem* 290: 2604–2616
 49. Reitz J, Gehrig-burger K, Ili JFS, Gimpl G (2008) Cholesterol interaction with the related steroidogenic acute regulatory lipid-transfer (START) domains of StAR (STARD1) and MLN64 (STARD3). *FEBS J* 64: 1790–1802
 50. Tsujishita Y, Hurley JH (2000) Structure and lipid transport mechanism of a StAR-related domain. *Nat Struct Biol* 7: 408–414
 51. Strushkevich N, MacKenzie F, Cherkasova T, Grabovec I, Usanov S, Park H-W (2011) Structural basis for pregnenolone biosynthesis by the mitochondrial monooxygenase system. *Proc Natl Acad Sci USA* 108: 10139–10143
 52. Rone MB, Midzak AS, Issop L, Rammouz G, Jagannathan S, Fan J, Ye X, Blonder J, Veenstra T, Papadopoulos V (2012) Identification of a dynamic mitochondrial protein complex driving cholesterol import, trafficking, and metabolism to steroid hormones. *Mol Endocrinol* 26: 1868–1882
 53. Liu J, Rone MB, Papadopoulos V (2006) Protein-protein interactions mediate mitochondrial cholesterol transport and steroid biosynthesis. *J Biol Chem* 281: 38879–38893
 54. Pulli I, Lassila T, Pan G, Yan D, Olkkonen VM, Törnquist K (2018) Oxysterol-binding protein related-proteins (ORPs) 5 and 8 regulate calcium signaling at specific cell compartments. *Cell Calcium* 72: 62–69
 55. Simmen T, Aslan JE, Blagoveshchenskaya AD, Thomas L, Wan L, Xiang Y, Feliciangeli SF, Hung CH, Crump CM, Thomas G (2005) PACS-2 controls endoplasmic reticulum-mitochondria communication and Bid-mediated apoptosis. *EMBO J* 24: 717–729
 56. Arif T, Krelm Y, Shoshan-Barmatz V (2016) Reducing VDAC1 expression induces a non-apoptotic role for pro-apoptotic proteins in cancer cell differentiation. *Biochim Biophys Acta* 1857: 1228–1242
 57. Gatiloff J, East DA, Singh A, Alvarez MS, Frison M, Matic I, Ferraina C, Sampson N, Turkheimer F, Campanella M (2017) A role for TSPO in mitochondrial Ca²⁺ homeostasis and redox stress signaling. *Cell Death Dis* 8: 1–15
 58. Friedman JR, Lackner LL, West M, DiBenedetto JR, Nunnari J, Voeltz GK (2011) ER tubules mark sites of mitochondrial division. *Science* 334: 358–362
 59. Korobova F, Ramabhadran V, Higgs HN (2013) An actin-dependent step in mitochondrial fission mediated by the ER-associated formin INF2. *Science* 339: 464–468
 60. Korobova F, Gauvin TJ, Higgs HN (2014) A role for myosin II in mammalian mitochondrial fission. *Curr Biol* 24: 409–414

61. Chakrabarti R, Ji WK, Stan RV, de Juan Sanz J, Ryan TA, Higgs HN (2018) INF2-mediated actin polymerization at the ER stimulates mitochondrial calcium uptake, inner membrane constriction, and division. *J Cell Biol* 217: 251–268
62. Loson OC, Song Z, Chen H, Chan DC (2013) Fis1, Mff, MiD49, and MiD51 mediate Drp1 recruitment in mitochondrial fission. *Mol Biol Cell* 24: 659–667
63. Yu R, Liu T, Jin S, Ning C, Lendahl U, Nistér M, Zhao J (2017) MIEF1/2 function as adaptors to recruit Drp1 to mitochondria and regulate the association of Drp1 with Mff. *Sci Rep* 7: 880
64. Kim Y, Youn S, Sudhakar V, Das A, Chandhri R, Cuervo Grajal H, Kweon J, Lehnart S, He L, Toth PT *et al* (2018) Redox regulation of mitochondrial fission protein Drp1 by protein disulfide isomerase limits endothelial senescence. *Cell Rep* 23: 3565–3578
65. Arasaki K, Shimizu H, Mogari H, Nishida N, Hirota N, Furuno A, Kudo Y, Baba M, Baba N, Cheng J *et al* (2015) A role for the ancient SNARE syntaxin 17 in regulating mitochondrial division. *Dev Cell* 32: 304–317
66. Rambold AS, Kostecky B, Elia N, Lippincott-Schwartz J (2011) Tubular network formation protects mitochondria from autophagosomal degradation during nutrient starvation. *Proc Natl Acad Sci USA* 108: 10190–10195
67. Lewis SC, Uchiyama LF, Nunnari J (2016) ER-mitochondria contacts couple mtDNA synthesis with mitochondrial division in human cells. *Science* 353: aaf5549
68. Wu W, Lin C, Wu K, Jiang L, Wang X, Li W, Zhuang H, Zhang X, Chen H, Li S *et al* (2016) FUNDC1 regulates mitochondrial dynamics at the ER-mitochondrial contact site under hypoxic conditions. *EMBO J* 35: 1368–1384
69. Chan DC (2006) Dissecting mitochondrial fusion. *Dev Cell* 11: 592–594
70. Anand R, Wai T, Baker MJ, Kladt N, Schauss AC, Rugarli E, Langer T (2014) The i-AAA protease YME1L and OMA1 cleave OPA1 to balance mitochondrial fusion and fission. *J Cell Biol* 204: 919–929
71. Yan L, Qi Y, Huang X, Yu C, Lan L, Guo X, Rao Z, Hu J, Lou Z (2018) Structural basis for GTP hydrolysis and conformational change of MFN1 in mediating membrane fusion. *Nat Struct Mol Biol* 25: 233–243
72. Franco A, Kitsis RN, Fleischer JA, Gavathiotis E, Kornfeld OS, Gong G, Biris N, Benz A, Qvit N, Donnelly SK *et al* (2016) Correcting mitochondrial fusion by manipulating mitofusin conformations. *Nature* 540: 74–79
73. Liu J, Noel JK, Low HH (2018) Structural basis for membrane tethering by a bacterial dynamin-like pair. *Nat Commun* 9: 1–12
74. Cerqua C, Anesti V, Pyakurel A, Liu D, Naon D, Wiche G, Baffa R, Dimmer KS, Scorrano L (2010) Trichoplein/mitostatin regulates endoplasmic reticulum-mitochondria juxtaposition. *EMBO Rep* 11: 854–860
75. Tian Y, Li B, Shi WZ, Chang MZ, Zhang GJ, Di ZL, Liu Y (2014) Dynamin-related protein 1 inhibitors protect against ischemic toxicity through attenuating mitochondrial Ca^{2+} uptake from endoplasmic reticulum store in PC12 cells. *Int J Mol Sci* 15: 3172–3185
76. Wu S, Lu Q, Wang Q, Ding Y, Ma Z, Mao X, Huang K, Xie Z, Zou MH (2017) Binding of FUN14 domain containing 1 with inositol 1,4,5-trisphosphate receptor in mitochondria-associated endoplasmic reticulum membranes maintains mitochondrial dynamics and function in hearts *in vivo*. *Circulation* 136: 2248–2266
77. Weaver D, Eisner V, Liu X, Várnai P, Hunyady L, Gross A, Hajnóczky G (2014) Distribution and apoptotic function of outer membrane proteins depend on mitochondrial fusion. *Mol Cell* 54: 870–878
78. Papanicolaou KN, Khairallah RJ, Ngho GA, Chikando A, Luptak I, O'Shea KM, Riley DD, Lugus JJ, Colucci WS, Lederer WJ *et al* (2011) Mitofusin-2 maintains mitochondrial structure and contributes to stress-induced permeability transition in cardiac myocytes. *Mol Cell Biol* 31: 1309–1328
79. Han SM, Tsuda H, Yang Y, Vibbert J, Cottee P, Lee SJ, Winek J, Haueter C, Bellen HJ, Miller MA (2012) Secreted VAPB/ALS8 major sperm protein domains modulate mitochondrial localization and morphology via growth cone guidance receptors. *Dev Cell* 22: 348–362
80. Rizzuto R, Pinton P, Carrington W, Fay FS, Fogarty KE, Lifshitz LM, Tuft RA, Pozzan T (1998) Close contacts with the endoplasmic reticulum as determinants of mitochondrial Ca^{2+} responses. *Science* 280: 1763–1766
81. Lytton J, Westlin M, Burk SE, Shull E, MacLennan H (1992) Functional comparisons between isoforms of the sarcoplasmic or endoplasmic reticulum family of calcium pumps. *J Biol Chem* 267: 14483–14489
82. Miller KK, Verma A, Snyder SH, Ross CA (1991) Localization of an endoplasmic reticulum calcium ATPase mRNA in rat brain by *in situ* hybridization. *Neuroscience* 43: 1–9
83. Giorgi C, Marchi S, Pinton P (2018) The machineries, regulation and cellular functions of mitochondrial calcium. *Nat Rev Mol Cell Biol* 19: 713–730
84. Filadi R, Leal NS, Schreiner B, Rossi A, Dentoni G, Pinho CM, Wiehager B, Cieri D, Calì T, Pizzo P *et al* (2018) TOM70 sustains cell bioenergetics by promoting IP3R3-mediated ER to mitochondria Ca^{2+} transfer. *Curr Biol* 28: 369–382.e6
85. Giorgio V, Bisetto E, Soriano ME, Dabbeni-sala F, Basso E, Petronilli V, Forte MA, Bernardi P, Lippe G (2009) Cyclophilin D modulates mitochondrial FOF1-ATP synthase by interacting with the lateral stalk of the complex. *J Biol Chem* 284: 33982–33988
86. Ong HL, Liu X, Sharma A, Hegde RS, Ambudkar IS (2007) Intracellular Ca^{2+} release via the ER translocon activates store-operated calcium entry. *Pflügers Arch Eur J Physiol* 453: 797–808
87. Giunti R, Gamberucci A, Fulceri R, Bánhegyi G, Benedetti A (2007) Both translocon and a cation channel are involved in the passive Ca^{2+} leak from the endoplasmic reticulum: a mechanistic study on rat liver microsomes. *Arch Biochem Biophys* 462: 115–121
88. Booth DM, Enyedi B, Geiszt M, Várnai P, Hajnóczky G (2016) Redox nanodomains are induced by and control calcium signaling at the ER-mitochondrial interface. *Mol Cell* 63: 240–248
89. Dong Z, Shanmugapriya S, Tomar D, Siddiqui N, Lynch S, Nemani N, Breves SL, Zhang X, Tripathi A, Palaniappan P *et al* (2017) Mitochondrial Ca^{2+} uniporter is a mitochondrial luminal redox sensor that augments MCU channel activity. *Mol Cell* 65: 1014–1028
90. Betz C, Stracka D, Prescianotto-baschong C, Frieden M, Demareux N, Hall MN (2013) mTOR complex 2-Akt signaling at mitochondria associated endoplasmic reticulum membranes (MAM) regulates mitochondrial physiology. *Proc Natl Acad Sci USA* 110: 12526–12534
91. Khan MT, Wagner L, Yule DI, Bhanumathy C, Joseph SK (2006) Akt kinase phosphorylation of inositol 1,4,5-trisphosphate receptors. *J Biol Chem* 281: 3731–3737
92. Szado T, Vanderheyden V, Parys JB, De Smedt H, Rietdorf K, Kotelevets L, Chastre E, Khan F, Landegren U, Söderberg O *et al* (2008) Phosphorylation of inositol 1,4,5-trisphosphate receptors by protein kinase B/Akt inhibits Ca^{2+} release and apoptosis. *Proc Natl Acad Sci USA* 105: 2427–2432
93. Schäuble N, Lang S, Jung M, Cappel S, Schorr S, Ulucan Ö, Linxweiler J, Dudek J, Blum R, Helms V *et al* (2012) BiP-mediated closing of the Sec61 channel limits Ca^{2+} leakage from the ER. *EMBO J* 31: 3282–3296
94. Golic I, Velickovic K, Markelic M, Stancic A, Jankovic A, Vucetic M, Otasevic V, Buzadzic B, Korac B, Korac A (2014) Calcium-induced

- alteration of mitochondrial morphology and mitochondrial-endoplasmic reticulum contacts in rat brown adipocytes. *Eur J Histochem* 58: 2377
95. Sehgal P, Szalai XP, Olesen XC, Praetorius XHA, Nissen XP, Christensen SB, Engedal XN, Møller JV (2017) Inhibition of the sarco/endoplasmic reticulum (ER) Ca^{2+} -ATPase by thapsigargin analogs induces cell death via ER Ca^{2+} depletion and the unfolded protein response. *J Biol Chem* 292: 19656–19673
 96. Gomez-Suaga P, Paillusson S, Miller CCJ (2017) ER-mitochondria signaling regulates autophagy. *Autophagy* 13: 1250–1251
 97. Muñoz JP, Ivanova S, Sánchez-Wandelmer J, Martínez-Cristóbal P, Noguera E, Sancho A, Díaz-Ramos A, Hernández-Alvarez MI, Sebastián D, Mauvezin C et al (2013) Mfn2 modulates the UPR and mitochondrial function via repression of PERK. *EMBO J* 32: 2348–2361
 98. Harding HP, Zhang Y, Zeng H, Novoa I, Lu PD, Calfon M, Sadri N, Yun C, Popko B, Paules R et al (2003) An integrated stress response regulates amino acid metabolism and resistance to oxidative stress. *Mol Cell* 11: 619–633
 99. Blais JJD, Filipenko V, Bi M, Harding HHP, Ron D, Koumenis C, Wouters BG, Bell JC (2004) Activating transcription factor 4 is translationally regulated by hypoxic stress. *Mol Cell Biol* 24: 7469–7482
 100. Liang S-H, Zhang W, McGrath BC, Zhang P, Cavener DR (2006) PERK (eIF2 α kinase) is required to activate the stress-activated MAPKs and induce the expression of immediate-early genes upon disruption of ER calcium homeostasis. *Biochem J* 393: 201–209
 101. Tessitore A, Martin MP, Sano R, Ma Y, Mann L, Ingrassia A, Laywell ED, Steindler DA, Hendershot LM, Azzo A (2004) GM1-ganglioside-mediated activation of the unfolded protein response causes neuronal death in a neurodegenerative gangliosidosis. *Mol Cell* 15: 753–766
 102. Kharroubi I, Ladrie L, Cardozo AK, Dogusan Z, Cnop M, Eizirik DL (2004) Free fatty acids and cytokines induce pancreatic b-cell apoptosis by different mechanisms: role of nuclear factor- κ B and endoplasmic reticulum stress. *Endocrinology* 145: 5087–5096
 103. Lai E, Bikopoulos G, Wheeler MB, Rozakis-adcock M, Volchuk A (2008) Differential activation of ER stress and apoptosis in response to chronically elevated free fatty acids in pancreatic beta-cells. *Am J Physiol Endocrinol Metab* 294: 540–550
 104. Sidrauski C, Chapman R, Walter P (1998) The unfolded protein response: an intracellular signalling pathway with many surprising features. *Trends Cell Biol* 8: 245–249
 105. Haynes CM, Titus EA, Cooper AA (2004) Degradation of misfolded proteins prevents ER-derived oxidative stress and cell death. *Mol Cell* 15: 767–776
 106. Hetz C, Saxena S (2017) ER stress and the unfolded protein response in neurodegeneration. *Nat Rev Neurol* 13: 477–491
 107. Harding HP, Novoa I, Zhang Y, Zeng H, Wek R, Schapira M, Ron D (2000) Regulated translation initiation controls stress-induced gene expression in mammalian cells. *Mol Cell* 6: 1099–1108
 108. Han J, Back SH, Hur J, Lin YH, Gildersleeve R, Shan J, Yuan CL, Krokowski D, Wang S, Hatzoglou M et al (2013) ER-stress-induced transcriptional regulation increases protein synthesis leading to cell death. *Nat Cell Biol* 15: 481–490
 109. Chen X, Shen J, Prywes R (2002) The luminal domain of ATF6 senses endoplasmic reticulum (ER) stress and causes translocation of ATF6 from the ER to the Golgi. *J Biol Chem* 277: 13045–13052
 110. Yamamoto K, Sato T, Matsui T, Sato M, Okada T, Yoshida H, Harada A, Mori K (2007) Transcriptional induction of mammalian ER quality control proteins is mediated by single or combined action of ATF6 α and XBP1. *Dev Cell* 13: 365–376
 111. Yoshida H, Matsui T, Yamamoto A, Okada T, Mori K (2001) XBP1 mRNA is induced by ATF6 and spliced by IRE1 in response to ER stress to produce a highly active transcription factor. *Cell* 107: 881–891
 112. Urano F, Urano F, Wang X, Bertolotti A, Zhang Y, Chung P, Harding HP, Ron D (2008) Coupling of stress in the ER to activation of JNK protein kinases by transmembrane protein kinase IRE1. *Science* 664: 664–667
 113. Hollien J, Weissman JS (2006) Decay of endoplasmic reticulum-localized mRNAs during the unfolded protein response. *Science* 313: 104–107
 114. Chami M, Oulès B, Szabadkai G, Tacine R, Rizzuto R, Paterlini-Bréchet P (2008) Role of SERCA1 truncated isoform in the proapoptotic calcium transfer from ER to mitochondria during ER stress. *Mol Cell* 32: 641–651
 115. Verfaillie T, Rubio N, Garg AD, Bultynck G, Rizzuto R, Decuypere JP, Piette J, Linehan C, Gupta S, Samali A et al (2012) PERK is required at the ER-mitochondrial contact sites to convey apoptosis after ROS-based ER stress. *Cell Death Differ* 19: 1880–1891
 116. Hetz C, Papa FR (2018) The unfolded protein response and cell fate control. *Mol Cell* 69: 169–181
 117. Bravo R, Vicencio JM, Parra V, Troncoso R, Munoz JP, Bui M, Quiroga C, Rodríguez AE, Verdejo HE, Ferreira J et al (2011) Increased ER – mitochondrial coupling promotes mitochondrial respiration and bioenergetics during early phases of ER stress Increased ER – mitochondrial coupling promotes mitochondrial respiration and bioenergetics during early phases of ER stress. *J Cell Sci* 124: 2143–2152
 118. Lee A, Scapa EF, Cohen DE, Glimcher LH (2008) Regulation of hepatic lipogenesis by the transcription factor XBP1. *Science* 320: 1492–1497
 119. Liu X, Henkel AS, LeCuyer BE, Hubchak SC, Schipma MJ, Zhang E, Green RM (2017) Hepatic deletion of X-box binding protein 1 impairs bile acid metabolism in mice. *J Lipid Res* 58: 504–511
 120. So JS, Hur KY, Tarrio M, Ruda V, Frank-Kamenetsky M, Fitzgerald K, Kotliarsky V, Lichtman AH, Iwakaki T, Glimcher LH et al (2012) Silencing of lipid metabolism genes through ire1 α -mediated mRNA decay lowers plasma lipids in mice. *Cell Metab* 16: 487–499
 121. Ngho GA, Papanicolaou KN, Walsh K (2012) Loss of mitofusin 2 promotes endoplasmic reticulum stress. *J Biol Chem* 287: 20321–20332
 122. Gkogkas C, Middleton S, Kremer AM, Wardrobe C, Hannah M, Gillingwater TH, Skehel P (2008) VAPB interacts with and modulates the activity of ATF6. *Hum Mol Genet* 17: 1517–1526
 123. Ng FWH, Nguyen M, Kwan T, Branton PE, Nicholson DW, Cromlish JA, Shore GC (1997) p28 Bap31, a Bcl-2/Bcl-XL – and procaspase-8-associated protein in the endoplasmic reticulum. *J Cell Biol* 139: 327–338
 124. Hirsch T, Marzo I, Kroemer G (1997) Role of the mitochondrial permeability transition pore in apoptosis. *Biosci Rep* 17: 67–76
 125. Schinzel AC, Takeuchi O, Huang Z, Fisher JK, Zhou Z, Rubens J, Hetz C, Danial NN, Moskowitz MA, Korsmeyer SJ (2005) Cyclophilin D is a component of mitochondrial permeability transition and mediates neuronal cell death after focal cerebral ischemia. *Proc Natl Acad Sci USA* 102: 12005–12010
 126. Namba T, Tian F, Chu K, Hwang SY, Yoon KW, Byun S, Hiraki M, Mandinova A, Lee SW (2013) CDIP1-BAP31 complex transduces apoptotic signals from endoplasmic reticulum to mitochondria under endoplasmic reticulum stress. *Cell Rep* 5: 331–339
 127. Peña-Blanco A, García-Sáez AJ (2018) Bax, Bak and beyond — mitochondrial performance in apoptosis. *FEBS J* 285: 416–431
 128. Korsmeyer SJ, Wei MC, Saito M, Weiler S, Oh KJ, Schlesinger PH (2000) Pro-apoptotic cascade activates BID, which oligomerizes BAK or BAX

- into pores that result in the release of cytochrome *c*. *Cell Death Differ* 7: 1166–1173
129. Li P, Nijhawan D, Budihardjo I, Srinivasula SM, Ahmad M, Alnemri ES, Wang X (1997) Cytochrome *c* and dATP-dependent formation of Apaf-1/caspase-9 complex initiates an apoptotic protease cascade. *Cell* 91: 479–489
 130. Bassik MC, Scorrano L, Oakes SA, Pozzan T, Korsmeyer SJ (2004) Phosphorylation of BCL-2 regulates ER Ca^{2+} homeostasis and apoptosis. *EMBO J* 23: 1207–1216
 131. Brooks C, Wei Q, Feng L, Dong G, Tao Y, Mei L, Xie Z, Dong Z (2007) Bak regulates mitochondrial morphology and pathology during apoptosis by interacting with mitofusins. *Proc Natl Acad Sci USA* 104: 11649–11654
 132. Hoppins S, Edlich F, Cleland MM, Banerjee S, McCaffery JM, Youle RJ (2011) The soluble form of bax regulates mitochondrial fusion via MFN2 homotypic complexes. *Mol Cell* 41: 150–160
 133. Lamb CA, Yoshimori T, Tooze SA (2013) The autophagosome: origins unknown, biogenesis complex. *Nat Rev* 14: 759–774
 134. Tanida I, Ueno T, Kominami E (2004) LC3 conjugation system in mammalian autophagy. *Int J Biochem Cell Biol* 36: 2503–2518
 135. Gomez-Suaga P, Paillusson S, Stoica R, Noble W, Hanger DP, Miller CCJ (2017) The ER-mitochondria tethering complex VAPB-PTPIP51 regulates autophagy. *Curr Biol* 27: 371–385
 136. Ge L, Schekman R (2014) The ER-Golgi intermediate compartment feeds the phagophore membrane. *Autophagy* 10: 170–172
 137. Appenzeller-Herzog C, Hauri H (2006) The ER-Golgi intermediate compartment (ERGIC): in search of its identity and function. *J Cell Sci* 119: 2173–2183
 138. Nascimbeni AC, Giordano F, Codogno P, Morel E, Dupont N, Grasso D, Maria I (2017) ER – plasma membrane contact sites contribute to autophagosome biogenesis by regulation of local PI3P synthesis. *EMBO J* 36: 2018–2033
 139. Shinjo S, Jiang S, Nameta M, Suzuki T, Kanai M, Nomura Y, Goda N (2017) Disruption of the mitochondria-associated ER membrane (MAM) plays a central role in palmitic acid-induced insulin resistance. *Exp Cell Res* 359: 86–93
 140. Park SW, Zhou Y, Lee J, Lee J, Ozcan U (2010) Sarco(endo)plasmic reticulum Ca^{2+} -ATPase 2b is a major regulator of endoplasmic reticulum stress and glucose homeostasis in obesity. *Proc Natl Acad Sci USA* 107: 19320–19325
 141. Fu S, Yang L, Li P, Hofmann O, Dicker L, Hide W, Lin X, Watkins SM, Ivanov AR (2011) Aberrant lipid metabolism disrupts calcium homeostasis causing liver endoplasmic reticulum stress in obesity. *Nature* 473: 528–531
 142. Tubbs E, Chanon S, Robert M, Bendridi N, Bidaux G, Chauvin MA, Ji-Cao J, Durand C, Gauvrit-Ramette D, Vidal H et al (2018) Disruption of mitochondria-associated endoplasmic reticulum membrane (MAM) integrity contributes to muscle insulin resistance in mice and humans. *Diabetes* 67: 636–650
 143. Bach D, Pich S, Soriano FX, Vega N, Baumgartner B, Oriola J, Daugaard JR, Lloberas J, Camps M, Zierath JR et al (2003) Mitofusin-2 determines mitochondrial network architecture and mitochondrial metabolism. A novel regulatory mechanism altered in obesity. *J Biol Chem* 278: 17190–17197
 144. Liu R, Jin P, Yu L, Wang Y, Han L, Shi T, Li X (2014) Impaired mitochondrial dynamics and bioenergetics in diabetic skeletal muscle. *PLoS One* 9: e92810
 145. Bach D, Naon D, Pich S, Soriano FX, Vega N, Rieusset J, Laville M, Guillet C, Boirie Y, Wallberg-henriksson H et al (2005) Expression of Mfn2, the charcot-marie-tooth neuropathy type 2A gene, in human skeletal muscle: effects of type 2 diabetes, obesity, weight loss, and the regulatory role of tumor necrosis factor alpha and interleukin-6. *Diabetes* 54: 2685–2693
 146. Gastaldi G, Russell A, Golay A, Giacobino JP, Habicht F, Barthassat V, Muzzin P, Bobbioni-Harsch E (2007) Upregulation of peroxisome proliferator-activated receptor gamma coactivator gene (PGC1A) during weight loss is related to insulin sensitivity but not to energy expenditure. *Diabetologia* 50: 2348–2355
 147. Hernández-Alvarez MI, Chiellini C, Manco M, Naon D, Liesa M, Palacín M, Mingrone G, Zorzano A (2009) Genes involved in mitochondrial biogenesis/function are induced in response to bilio-pancreatic diversion in morbidly obese individuals with normal glucose tolerance but not in type 2 diabetic patients. *Diabetologia* 52: 1618–1627
 148. Mingrone G, Manco M, Calvani M, Castagneto M, Naon D, Zorzano A (2005) Could the low level of expression of the gene encoding skeletal muscle mitofusin-2 account for the metabolic inflexibility of obesity? *Diabetologia* 48: 2108–2114
 149. Hernández-Alvarez MI, Thabit H, Burns N, Shah S, Brema I, Hatunic M, Finucane F, Liesa M, Chiellini C, Naon D et al (2010) Subjects with early-onset type 2 diabetes show defective activation of the skeletal. *Diabetes Care* 33: 645–651
 150. Yang C, Aye CC, Li X, Diaz Ramos A, Zorzano A, Mora S (2012) Mitochondrial dysfunction in insulin resistance: differential contributions of chronic insulin and saturated fatty acid exposure in muscle cells. *Biosci Rep* 32: 465–478
 151. Wold LE, Dutta K, Mason MM, Ren J, Cala SE, Schwanke ML, Davidoff AJ (2005) Impaired SERCA function contributes to cardiomyocyte dysfunction in insulin resistant rats. *J Mol Cell Cardiol* 39: 297–307
 152. Thivolet C, Vial G, Cassel R, Rieusset J, Madec A-M (2017) Reduction of endoplasmic reticulum mitochondria interactions in beta cells from patients with type 2 diabetes. *PLoS One* 12: e0182027
 153. Zhang E, Mohammed Al-Amily I, Mohammed S, Luan C, Asplund O, Ahmed M, Ye Y, Ben-Hail D, Soni A, Vishnu N et al (2018) Preserving insulin secretion in diabetes by inhibiting VDAC1 overexpression and surface translocation in β cells. *Cell Metab* 29: 64–77
 154. Ahmed M, Muhammed SJ, Kessler B, Salehi A (2010) Mitochondrial proteome analysis reveals altered expression of voltage dependent anion channels in pancreatic β -cells exposed to high glucose. *Islets* 2: 283–292
 155. McKenzie MD, Jamieson E, Jansen ES, Scott CL, Huang DCS, Bouillet P, Allison J, Kay TWH, Strasser A, Thomas HE (2010) Glucose induces pancreatic islet cell apoptosis that requires the BH3-only proteins bim and puma and multi-bh domain protein bax. *Diabetes* 59: 644–652
 156. Schneeberger M, Dietrich MO, Sebastián D, Imbernón M, Castaño C, García A, Esteban Y, Gonzalez-Franquesa A, Rodríguez IC, Bortolozzi A et al (2013) Mitofusin 2 in POMC neurons connects ER stress with leptin resistance and energy imbalance. *Cell* 155: 172–187
 157. Filippi BM, Abraham MA, Silva PN, Rasti M, LaPierre MP, Bauer PV, Rocheleau JV, Lam TKT (2017) Dynamin-related protein 1-dependent mitochondrial fission changes in the dorsal vagal complex regulate insulin action. *Cell Rep* 18: 2301–2309
 158. Zhao L, Lu T, Gao L, Fu X, Zhu S, Hou Y (2017) Enriched endoplasmic reticulum-mitochondria interactions result in mitochondrial dysfunction and apoptosis in oocytes from obese mice. *J Anim Sci Biotechnol* 8: 1–8
 159. Sood A, Vijey D, Prudent J, Caron A, Lemieux P, McBride HM, Laplante M, Tóth K, Pellegrini L (2014) A mitofusin-2 – dependent inactivating

- cleavage of Opa1 links changes in mitochondria cristae and ER contacts in the postprandial liver. *Proc Natl Acad Sci USA* 111: 16017–16022
160. Theurey P, Tubbs E, Vial G, Jacquemetton J, Bendridi N, Chauvin MA, Alam MR, Le Romancer M, Vidal H, Rieusset J (2016) Mitochondria-associated endoplasmic reticulum membranes allow adaptation of mitochondrial metabolism to glucose availability in the liver. *J Mol Cell Biol* 8: 129–143
 161. Báez-Ruiz A, Cázarez-Gómez K, Vázquez-Martínez O, Aguilar-Roblero R, Díaz-Muñoz M (2013) Diurnal and nutritional adjustments of intracellular Ca^{2+} release channels and Ca^{2+} ATPases associated with restricted feeding schedules in the rat liver. *J Circadian Rhythms* 11: 1–17
 162. Levine B (2005) Eating oneself and uninvited guests: autophagy-related pathways in cellular defense. *Cell* 120: 159–162
 163. Hailey DW, Rambold AS, Satpute-Krishnan P, Mitra K, Sougrat R, Kim PK, Lippincott-Schwartz J (2010) Mitochondria supply membranes for autophagosome biogenesis during starvation. *Cell* 141: 656–667
 164. Mihai AD, Schröder M (2015) Glucose starvation and hypoxia, but not the saturated fatty acid palmitic acid or cholesterol, activate the unfolded protein response in 3T3-F442A and 3T3-L1 adipocytes. *Adipocyte* 4: 188–202
 165. Shao M, Shan B, Liu Y, Deng Y, Yan C, Wu Y, Mao T, Qiu Y, Zhou Y, Jiang S et al (2014) Hepatic IRE1 α regulates fasting-induced metabolic adaptive programs through the XBP1s-PPAR α axis signalling. *Nat Commun* 5: 3528
 166. Sebastian D, Hernandez-Alvarez MI, Segales J, Sorianoello E, Munoz JP, Sala D, Waget A, Liesa M, Paz JC, Gopalacharyulu P et al (2012) Mitofusin 2 (Mfn2) links mitochondrial and endoplasmic reticulum function with insulin signaling and is essential for normal glucose homeostasis. *Proc Natl Acad Sci USA* 109: 5523–5528
 167. Sebastián D, Sorianoello E, Segalés J, Irazoki A, Ruiz-Bonilla V, Sala D, Planet E, Berenguer-Llengo A, Muñoz JP, Sánchez-Feutrie M et al (2016) Mfn2 deficiency links age-related sarcopenia and impaired autophagy to activation of an adaptive mitophagy pathway. *EMBO J* 35: 1677–1693
 168. Kulkarni SS, Joffraud M, Boutant M, Ratajczak J, Gao AW, MacLachlan C, Hernandez Alvarez MI, Raymond F, Metairon S, Descombes P et al (2016) Mfn1 deficiency in the liver protects against diet-induced insulin resistance and enhances the hypoglycemic effect of metformin. *Diabetes* 65: 3552–3560
 169. Mahdavian K, Benador IY, Su S, Gharakhanian RA, Stiles L, Trudeau KM, Cardamone M, Enríquez-Zarralanga V, Ritou E, Aprahamian T et al (2017) Mfn2 deletion in brown adipose tissue protects from insulin resistance and impairs thermogenesis. *EMBO Rep* 18: 1123–1138
 170. Dietrich MO, Liu ZW, Horvath TL (2013) Mitochondrial dynamics controlled by mitofusins regulate agrp neuronal activity and diet-induced obesity. *Cell* 155: 188–199
 171. Ramírez S, Gómez-Valadés AG, Schneeberger M, Varela L, Haddad-Tóvolli R, Altirriba J, Noguera E, Drougard A, Flores-Martínez Á, Imbernón M et al (2017) Mitochondrial dynamics mediated by mitofusin 1 is required for POMC neuron glucose-sensing and insulin release control. *Cell Metab* 25: 1390–1399.e6
 172. Starenki D, Hong SK, Lloyd RV, Park JI (2015) Mortalin (GRP75/HSPA9) upregulation promotes survival and proliferation of medullary thyroid carcinoma cells. *Oncogene* 34: 4624–4634
 173. Burbulla LF, Fitzgerald JC, Stegen K, Westermeier J, Thost AK, Kato H, Mokranjac D, Sauerwald J, Martins LM, Voitalla D et al (2014) Mitochondrial proteolytic stress induced by loss of mortalin function is rescued by Parkin and PINK1. *Cell Death Dis* 5: 1–19
 174. Xu J-L, Li L-Y, Wang Y-Q, Li Y-Q, Shan M, Sun S-Z, Yu Y, Wang B (2018) Hepatocyte-specific deletion of BAP31 promotes SREBP1C activation, promotes hepatic lipid accumulation, and worsens IR in mice. *J Lipid Res* 59: 35–47
 175. Wu Z, Yang F, Jiang S, Sun X, Xu J (2018) Induction of liver steatosis in BAP31-deficient mice burdened with tunicamycin-induced endoplasmic reticulum stress. *Int J Mol Sci* 19: 1–16
 176. Rieusset J, Fauconnier J, Paillard M, Belaidi E, Tubbs E, Chauvin M, Durand A, Bravard A, Teixeira G, Bartosch B et al (2016) Disruption of calcium transfer from ER to mitochondria links alterations of mitochondria-associated ER membrane integrity to hepatic insulin resistance. *Diabetologia* 59: 614–623
 177. Özcan U, Cao Q, Yilmaz E, Lee A-H, Iwakoshi NN, Özdelin E, Tuncman G, Görgün C, Glimcher LH, Hotamisligil GS (2004) Endoplasmic reticulum stress links obesity, insulin action, and type 2 diabetes. *Science* 306: 457–461
 178. Baiceanu A, Mesdom P, Lagouge M, Fougelle F (2016) Endoplasmic reticulum proteostasis in hepatic steatosis. *Nat Rev Endocrinol* 12: 710–722
 179. Frakes AE, Dillin A (2017) The UPRER: sensor and coordinator of organismal homeostasis. *Mol Cell* 66: 761–771
 180. Shpilka T, Haynes CM (2018) The mitochondrial UPR: mechanisms, physiological functions and implications in ageing. *Nat Rev Mol Cell Biol* 19: 109–120
 181. Chen KH, Dasgupta A, Ding J, Indig FE, Ghosh P, Longo DL (2014) Role of mitofusin 2 (Mfn2) in controlling cellular proliferation. *FASEB J* 28: 382–394
 182. de Brito OM, Scorrano L (2009) Mitofusin-2 regulates mitochondrial and endoplasmic reticulum morphology and tethering: the role of Ras. *Mitochondrion* 9: 222–226
 183. Klawitter J, Seres T, Pennington A, Beatty JT, Klawitter J, Christians U (2017) Ablation of cyclophilin D results in an activation of FAK, Akt, and ERK pathways in the mouse heart. *J Cell Biochem* 118: 2933–2940
 184. Kim W-T, Choi HS, Lee HM, Jang Y-J, Ryu CJ (2014) B-cell receptor-associated protein 31 regulates human embryonic stem cell adhesion, stemness, and survival via control of epithelial cell adhesion molecule. *Stem Cells* 32: 2626–2641
 185. Choi JH, Banks AS, Estall JL, Kajimura S, Boström P, Laznik D, Ruas JL, Chalmers MJ, Kamenecka TM, Blüher M et al (2010) Anti-diabetic drugs inhibit obesity-linked phosphorylation of PPAR γ 3 by Cdk5. *Nature* 466: 451–456
 186. Banks AS, McAllister FE, Camporez JPC, Zushin PJH, Jurczak MJ, Laznik-Bogoslavski D, Shulman GI, Gygi SP, Spiegelman BM (2015) An ERK/Cdk5 axis controls the diabetogenic actions of PPAR γ . *Nature* 517: 391–395
 187. Fu T, Xu Z, Liu L, Guo Q, Wu H, Liang X, Zhou D, Xiao L, Liu L, Liu Y et al (2018) Mitophagy directs muscle-adipose crosstalk to alleviate dietary obesity. *Cell Rep* 23: 1357–1372
 188. Krzysiek TC, Thomas L, Choi Y, Auclair S, Qian Y, Luan S, Krasnow SM, Thomas LL, Koharudin LMI, Benos PV et al (2018) An insulin-responsive sensor in the SIRT1 disordered region binds DBC1 and PACS-2 to control enzyme activity. *Mol Cell* 72: 985–998.e7
 189. Potthoff MJ (2017) FGF21 and metabolic disease in 2016: a new frontier in FGF21 biology. *Nat Rev Endocrinol* 13: 74–76
 190. Kharitonov A, Shiyanova TL, Koester A, Ford AM, Micanovic R, Galbreath EJ, Sandusky GE, Hammond LJ, Moyers JS, Owens RA et al

- (2005) FGF-21 as a novel metabolic regulator. *J Clin Invest* 115: 1627–1635
191. Luciani DS, White SA, Widenmaier SB, Saran VV, Taghizadeh F, Hu X, Allard MF, Johnson JD (2013) Bcl-2 and Bcl-xl suppress glucose signaling in pancreatic b-cells. *Diabetes* 62: 170–182
 192. Liu X, Li L, Li J, Cheng Y, Chen J (2016) Insulin resistance contributes to multidrug resistance in HepG2 cells via activation of the PERK signaling pathway and upregulation of Bcl-2 and P-gp. *Oncol Rep* 35: 3018–3024
 193. Ye R, Ni M, Wang M, Luo S, Zhu G, Chow RH, Lee AS (2011) Inositol 1,4,5-trisphosphate receptor 1 mutation perturbs glucose homeostasis and enhances susceptibility to diet-induced diabetes. *J Endocrinol* 210: 209–217
 194. Arif T, Paul A, Krelin Y, Shteinfein-Kuzmine A, Shoshan-Barmatz V (2018) Mitochondrial VDAC1 silencing leads to metabolic rewiring and the reprogramming of tumour cells into advanced differentiated states. *Cancers (Basel)* 10: E499
 195. Arif T, Krelin Y, Nakdimon I, Benharroch D, Paul A, Dadon-Klein D, Shoshan-Barmatz V (2017) VDAC1 is a molecular target in glioblastoma, with its depletion leading to reprogrammed metabolism and reversed oncogenic properties. *Neuro Oncol* 19: 951–964
 196. Chen H, Gao W, Yang Y, Guo S, Wang H, Wang W, Zhang S, Zhou Q, Xu H, Yao J et al (2014) Inhibition of VDAC1 prevents Ca²⁺-mediated oxidative stress and apoptosis induced by 5-aminolevulinic acid mediated sonodynamic therapy in THP-1 macrophages. *Apoptosis* 19: 1712–1726
 197. Lamming DW, Ye L, Katajisto P, Goncalves MD, Saitoh M, Stevens DM, Davis JG, Salmon AB, Richardson A, Ahima RS et al (2012) Rapamycin-induced insulin resistance is mediated by mTORC2 loss and uncoupled from longevity. *Science* 335: 1638–1643
 198. Peralta S, Goffart S, Williams SL, Diaz F, Garcia S, Nissanka N, Area-Gomez E, Pohjoismäki J, Moraes CT (2018) ATAD3 controls mitochondrial cristae structure in mouse muscle, influencing mtDNA replication and cholesterol levels. *J Cell Sci* 131: jcs217075
 199. Desai R, Frazier AE, Durigon R, Patel H, Jones AW, Rosa ID, Lake NJ, Compton AG, Mountford HS, Tucker EJ et al (2017) ATAD3 gene cluster deletions cause cerebellar dysfunction associated with altered mitochondrial DNA and cholesterol metabolism. *Brain* 140: 1595–1610
 200. Issop L, Fan J, Lee S, Rone MB, Basu K, Mui J, Papadopoulos V (2015) Mitochondria-associated membrane formation in hormone-stimulated leydig cell steroidogenesis: role of ATAD3. *Endocrinology* 156: 334–345
 201. Beaslas O, Metso J, Nissila E, Laurila PP, Kaiharju E, Batchu KC, Kaipainen L, Mayranpää MI, Yan D, Gylling H et al (2013) Osbp18 deficiency in mouse causes an elevation of high-density lipoproteins and gender-specific alterations of lipid metabolism. *PLoS One* 8: e58856
 202. Wang H, Sreenivasan U, Gong D-W, O'Connell KA, Dabkowski ER, Hecker PA, Ionica N, Konig M, Mahurkar A, Sun Y et al (2013) Cardiomyocyte-specific perilipin 5 overexpression leads to myocardial steatosis and modest cardiac dysfunction. *J Lipid Res* 54: 953–965
 203. Tarnopolsky MA, Rennie CD, Robertshaw HA, Fedak-Tarnopolsky SN, Devries MC, Hamadeh MJ (2006) Influence of endurance exercise training and sex on intramyocellular lipid and mitochondrial ultrastructure, substrate use, and mitochondrial enzyme activity. *Am J Physiol Regul Integr Comp Physiol* 292: R1271–R1278
 204. Shiozaki M, Hayakawa N, Shibata M, Koike M, Uchiyama Y, Gotow T (2011) Closer association of mitochondria with lipid droplets in hepatocytes and activation of Kupfer cells in resveratrol-treated senescence-accelerated mice. *Histochem Cell Biol* 136: 475–489
 205. Yu J, Zhang S, Cui L, Wang W, Na H, Zhu X, Li L, Xu G, Yang F, Christian M et al (2015) Lipid droplet remodeling and interaction with mitochondria in mouse brown adipose tissue during cold treatment. *Biochim Biophys Acta* 1853: 918–928
 206. Rambold AS, Cohen S, Lippincott-Schwartz J (2015) Fatty acid trafficking in starved cells: regulation by lipid droplet lipolysis, autophagy, and mitochondrial fusion dynamics. *Dev Cell* 32: 678–692
 207. Nguyen TB, Louie SM, Daniele JR, Tran Q, Dillin A, Zoncu R, Nomura DK, Olzmann JA (2017) DGAT1-dependent lipid droplet biogenesis protects mitochondrial function during starvation-induced autophagy. *Dev Cell* 42: 9–21.e5
 208. Cahill GF (1970) Starvation in man. *N Engl J Med* 282: 668–675
 209. Young PA, Senkal CE, Suchanek AL, Grevengoed TJ, Lin DD, Zhao L, Crunk AE, Klett EL, Füllekrug J, Obeid LM et al (2018) Long-chain acyl-CoA synthetase 1 interacts with key proteins that activate and direct fatty acids into niche hepatic pathways. *J Biol Chem* 293: 16724–16740
 210. Jägerström S, Polesie S, Wickström Y, Johansson BR, Schröder HD, Højlund K, Boström P (2009) Lipid droplets interact with mitochondria using SNAP23. *Cell Biol Int* 33: 934–940
 211. Boström P, Andersson L, Rutberg M, Perman J, Lidberg U, Johansson BR, Fernandez-Rodriguez J, Ericson J, Nilsson T, Borén J et al (2007) SNARE proteins mediate fusion between cytosolic lipid droplets and are implicated in insulin sensitivity. *Nat Cell Biol* 9: 1286–1293
 212. Wang H, Sreenivasan U, Hu H, Saladino A, Polster BM, Lund LM, Gong D, Stanley WC, Szataly C (2011) Perilipin 5, a lipid droplet-associated protein, provides physical and metabolic linkage to mitochondria. *J Lipid Res* 52: 2159–2168
 213. Bosma M, Minnaard R, Sparks LM, Schaart G, Losen M, De Baets MH, Duimel H, Kersten S, Bickel PE, Schrauwen P et al (2012) The lipid droplet coat protein perilipin 5 also localizes to muscle mitochondria. *Histochem Cell Biol* 137: 205–216
 214. Granneman JG, Moore HPH, Mottillo EP, Zhu Z, Zhou L (2011) Interactions of Perilipin-5 (Plin5) with adipose triglyceride lipase. *J Biol Chem* 286: 5126–5135
 215. Calderon-Dominguez M, Mir JF, Fucho R, Weber M, Serra D, Herrero L (2016) Fatty acid metabolism and the basis of brown adipose tissue function. *Adipocyte* 5: 98–118
 216. Herms A, Bosch M, Reddy BJN, Schieber NL, Fajardo A, Ruperez C, Fernandez-Vidal A, Ferguson C, Rentero C, Tebar F et al (2015) AMPK activation promotes lipid droplet dispersion on dephosphorylated microtubules to increase mitochondrial fatty acid oxidation. *Nat Commun* 6: 1–14
 217. Sath K, Rai P, Mallik R (2017) Feeding-fasting dependent recruitment of membrane microdomain proteins to lipid droplets purified from the liver. *PLoS One* 12: e0183022
 218. Kramer DA, Quiroga AD, Lian J, Fahlman RP, Lehner R (2018) Fasting and refeeding induces changes in the mouse hepatic lipid droplet proteome. *J Proteomics* 181: 213–224
 219. Sohn JH, Lee YK, Han JS, Jeon YG, Kim JI, Choe SS, Kim SJ, Yoo HJ, Kim JB (2018) Perilipin 1 (Plin1) deficiency promotes inflammatory responses in lean adipose tissue through lipid dysregulation. *J Biol Chem* 293: 13974–13988
 220. Laurens C, Bourlier V, Mairal A, Louche K, Badin PM, Mouisel E, Montagner A, Marette A, Tremblay A, Weisnagel JS et al (2016) Perilipin 5 fine-tunes lipid oxidation to metabolic demand and protects against lipotoxicity in skeletal muscle. *Sci Rep* 6: 1–12

221. Morton TL, Galior K, McGrath C, Wu X, Uzer G, Uzer GB, Sen B, Xie Z, Tyson D, Rubin J et al (2016) Exercise increases and browns muscle lipid in high-fat diet-fed mice. *Front Endocrinol (Lausanne)* 7: 1–8
222. Gemmink A, Daemen S, Brouwers B, Huntjens PR, Schaart G, Moonen-Kornips E, Jörgensen J, Hoeks J, Schrauwen P, Hesselink MKC (2018) Dissociation of intramyocellular lipid storage and insulin resistance in trained athletes and type 2 diabetes patients; involvement of perilipin 5? *J Physiol* 596: 857–868
223. Covington JD, Noland RC, Hebert RC, Masinter BS, Smith SR, Rustan AC, Ravussin E, Bajpeyi S (2015) Perilipin 3 differentially regulates skeletal muscle lipid oxidation in active, sedentary, and type 2 diabetic males. *J Clin Endocrinol Metab* 100: 3683–3692
224. Keenan SN, Meex RC, Lo JCY, Ryan A, Nie S, Magdalene K (2019) Perilipin 5 deletion in hepatocytes remodels lipid metabolism and causes hepatic insulin resistance in mice. *Diabetes* 68: 543–555
225. Montgomery MK, Mokhtar R, Bayliss J, Parkington HC, Suturin VM, Bruce CR, Watt MJ (2018) Perilipin 5 deletion unmasks an endoplasmic reticulum Stress-Fibroblast growth factor 21 axis in skeletal muscle. *Diabetes* 67: 594–606
226. Harris LALS, Skinner JR, Shew TM, Pietka TA, Abumrad NA, Wolins NE (2015) Perilipin 5-driven lipid droplet accumulation in skeletal muscle stimulates the expression of fibroblast growth factor 21. *Diabetes* 64: 2757–2768
227. Wei S, Liu S, Su X, Wang W, Li F, Deng J, Lyu Y, Geng B, Xu G (2018) Spontaneous development of hepatosteatosis in perilipin-1 null mice with adipose tissue dysfunction. *Biochim Biophys Acta* 1863: 212–218
228. Liu S, Geng B, Zou L, Wei S, Wang W, Deng J, Xu C, Zhao X, Lyu Y, Su X et al (2015) Development of hypertrophic cardiomyopathy in perilipin-1 null mice with adipose tissue dysfunction. *Cardiovasc Res* 105: 20–30
229. Langlois D, Forcheron F, Li JY, Del Carmine P, Neggazi S, Beylot M (2011) Increased atherosclerosis in mice deficient in perilipin1. *Lipids Health Dis* 10: 1–6
230. Nguyen TN, Padman BS, Lazarou M (2016) Deciphering the molecular signals of PINK1/parkin mitophagy. *Trends Cell Biol* 26: 733–744
231. Sugiura A, McLelland G, Fon EA, McBride HM (2014) A new pathway for mitochondrial quality control: mitochondrial-derived vesicles. *EMBO J* 33: 2142–2156
232. Raimundo N, Fernández-mosquera L, Yambire KF, Diogo CV (2016) Mechanisms of communication between mitochondria and lysosomes. *Int J Biochem Cell Biol* 79: 345–349
233. Han Y, Li M, Qiu F, Zhang M, Zhang Y-H (2017) Cell-permeable organic fluorescent probes for live-cell long-term super-resolution imaging reveal lysosome-mitochondrion interactions. *Nat Commun* 8: 1307–1316
234. Zhao T, Huang X, Han L, Wang X, Cheng H, Zhao Y, Chen Q, Chen J, Cheng H, Xiao R et al (2012) Central role of mitofusin 2 in autophagosome-lysosome fusion in cardiomyocytes. *J Biol Chem* 287: 23615–23625
235. Cioni J, Lin JQ, Holtermann AV, Franze K, Harris WA, Holt CE, Cioni J, Lin JQ, Holtermann AV, Koppers M et al (2019) Late endosomes act as mRNA translation platforms and sustain mitochondria in axons article late endosomes act as mRNA translation platforms and sustain mitochondria in axons. *Cell* 176: 56–72.e15
236. Muñoz-Bracerás S, Tornero-Écija AR, Vincent O, Escalante R (2019) VPS13A is closely associated with mitochondria and is required for efficient lysosomal degradation. *Dis Model Mech* 12: 1–13
237. Zhang X, Walsh B, Mitchell CA, Rowe T (2005) TBC domain family, member 15 is a novel mammalian Rab GTPase-activating protein with substrate preference for Rab7. *Biochem Biophys Res Commun* 335: 154–161
238. Kumar N, Leonzino M, Cerutti WH, Horenkamp FA, Li P, Lees JA (2018) VPS13A and VPS13C are lipid transport proteins differentially localized at ER contact sites. *J Cell Biol* 217: 3625–3639
239. Itoh K, Adachi Y, Yamada T, Suzuki TL, Otomo T, McBride HM, Yoshimori T, Iijima M, Sesaki H (2018) A brain-enriched Drp1 isoform associates with lysosomes, late endosomes, and the plasma membrane. *J Biol Chem* 293: 11809–11822
240. Kon K, Kim J, Uchiyama A, Jaeschke H, Lemasters JJ (2010) Lysosomal iron mobilization and induction of the mitochondrial permeability transition in acetaminophen-induced toxicity to mouse hepatocytes. *Toxicol Sci* 117: 101–108
241. König J, Ott C, Hugo M, Jung T (2017) Mitochondrial contribution to lipofuscin formation. *Redox Biol* 11: 673–681
242. Mukhopadhyay A, Pan X, Lambright DG, Tissenbaum HA (2007) An endocytic pathway as a target of tubby for regulation of fat storage. *EMBO Rep* 8: 931–938
243. Ding X, Zhang W, Zhao T, Yan C, Du H (2017) Rab7 GTPase controls lipid metabolic signaling in myeloid- derived suppressor cells. *Oncotarget* 8: 30123–30137
244. Wu J, Cheng D, Liu L, Lv Z, Liu K (2019) TBC1D15 affects glucose uptake by regulating GLUT4 translocation. *Gene* 683: 210–215
245. Hönscher C, Mari M, Auffarth K, Bohnert M, Griffith J, Geerts W, Van Der Laan M (2014) Cellular metabolism regulates contact sites between vacuoles and mitochondria. *Dev Cell* 30: 86–94
246. Gonzalez Montoro A, Kathrin A, Honscher C, Bohnert M, Becker T, Warscheid B, Reggiori F, van der Laan M, Frohlich F, Ungermann C (2018) Vps39 interacts with Tom40 to establish one of two functionally distinct vacuole-mitochondria contact sites. *Dev Cell* 45: 621–636
247. Norambuena A, Wallrabe H, Cao R, Wang DB, Silva A, Svindrych Z, Periasamy A, Hu S, Tanzi RE, Kim DY et al (2018) A novel lysosome-to-mitochondria signaling pathway disrupted by amyloid- b oligomers. *EMBO J* 37: 1–18
248. Islinger M, Lüers GH, Zischka H, Ueffing M, Völkl A (2006) Insights into the membrane proteome of rat liver peroxisomes: microsomal glutathione-S-transferase is shared by both subcellular compartments. *Proteomics* 6: 804–816
249. Horner SM, Wilkins C, Badil S, Iskarpatyoti J (2015) Proteomic analysis of mitochondrial-associated ER membranes (MAM) during RNA virus infection reveals dynamic changes in protein and organelle trafficking. *PLoS One* 10: e0117963
250. Horner SM, Liu HM, Park HS, Briley J, Gale M (2011) Mitochondrial-associated membranes (MAM) form innate immune synapses and are targeted by hepatitis C virus. *Proc Natl Acad Sci USA* 108: 14590–14595
251. Schrader M, Costello J, Godinho LF, Islinger M (2015) Peroxisome-mitochondria interplay and disease. *J Inherit Metab Dis* 38: 681–702
252. Otera H, Mihara K (2011) Discovery of the membrane receptor for mitochondrial fission GTPase Drp1. *Small GTPases* 2: 167–172
253. Kirichok Y, Krapivinsky G, Clapham DE (2004) The mitochondrial calcium uniporter is a highly selective ion channel. *Nature* 427: 360–364